

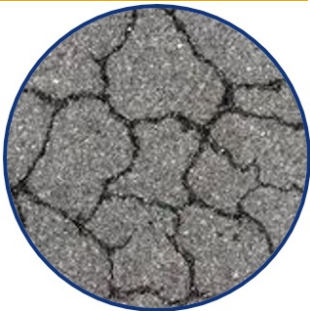


Prediction and Rehabilitation of Highway Embankment Slope Failures in Changing Climate

Project No. 17GTL SU04

Lead University: Louisiana State University

Collaborative Universities: University of Texas at Arlington



Enhancing Durability and Service Life of Infrastructure

Disclaimer

The contents of this report reflect the views of the authors, who are responsible for the facts and the accuracy of the information presented herein. This document is disseminated in the interest of information exchange. The report is funded, partially or entirely, by a grant from the U.S. Department of Transportation's University Transportation Centers Program. However, the U.S. Government assumes no liability for the contents or use thereof.

Acknowledgments

The discussions and feedback by the Louisiana Department of Transportation and Development are greatly appreciated.

TECHNICAL DOCUMENTATION PAGE

1. Project No. 17GTLSU04	2. Government Accession No.	3. Recipient's Catalog No.	
4. Title and Subtitle Prediction and Rehabilitation of Highway Embankment Slope Failures in a Changing Climate		5. Report Date Oct. 2018	
7. Author(s) PI: Navid H. Jafari https://orcid.org/0000-0002-4394-3776 Co-PI: Anand J. Puppala https://orcid.org/0000-0003-0435-6285		6. Performing Organization Code	
9. Performing Organization Name and Address Transportation Consortium of South-Central States (Tran-SET) University Transportation Center for Region 6 3319 Patrick F. Taylor Hall, Louisiana State University, Baton Rouge, LA 70803		8. Performing Organization Report No.	
12. Sponsoring Agency Name and Address United States of America Department of Transportation Research and Innovative Technology Administration		10. Work Unit No. (TRAIS)	
		11. Contract or Grant No. 69A3551747106	
		13. Type of Report and Period Covered Final Research Report May 2017 – May 2018	
		14. Sponsoring Agency Code	
15. Supplementary Notes Report uploaded and accessible at: Tran-SET's website (http://transet.lsu.edu/)			
16. Abstract Highway slopes constructed with clayey soil are prone to desiccation cracks due to wetting and drying weather cycle, which allows greater moisture infiltration into the embankment from precipitation. Fissures formed due to extended wetting and drying cycles allow water to seep deeper into the soil than surficial wetting and increase the water content. This increases the moisture content in the soil and results in reduction in shear strength to the fully softened strength. On the other hand, development of desiccation cracks and reduction of the soil matric suction ultimately result in higher hydraulic conductivity value which causes development of higher pore water pressure. As the moisture content of the clayey soil increases, the strength reduces to a fully softened shear strength that causes frequent shallow and medium slope failures that are oriented approximately parallel to the surface of the embankment. Hence, the fully softened strength of Louisiana and Texas soils need to be quantified to develop a predictive tool for identifying high-risk zones of highway embankments. Given the documented failures in Texas and Louisiana, this research project is focused on investigating past failures to develop lessons learned and guidelines that can be implemented in the predictive framework.			
17. Key Words Shallow slope failure, Fully softened strength, Soil water retention curve, Climate change		18. Distribution Statement No restrictions.	
19. Security Classif. (of this report) Unclassified	20. Security Classif. (of this page) Unclassified	21. No. of Pages 34	22. Price

Form DOT F 1700.7 (8-72)

Reproduction of completed page authorized.

SI* (MODERN METRIC) CONVERSION FACTORS

APPROXIMATE CONVERSIONS TO SI UNITS

Symbol	When You Know	Multiply By	To Find	Symbol
LENGTH				
in	inches	25.4	millimeters	mm
ft	feet	0.305	meters	m
yd	yards	0.914	meters	m
mi	miles	1.61	kilometers	km
AREA				
in ²	square inches	645.2	square millimeters	mm ²
ft ²	square feet	0.093	square meters	m ²
yd ²	square yard	0.836	square meters	m ²
ac	acres	0.405	hectares	ha
mi ²	square miles	2.59	square kilometers	km ²
VOLUME				
fl oz	fluid ounces	29.57	milliliters	mL
gal	gallons	3.785	liters	L
ft ³	cubic feet	0.028	cubic meters	m ³
yd ³	cubic yards	0.765	cubic meters	m ³
NOTE: volumes greater than 1000 L shall be shown in m ³				
MASS				
oz	ounces	28.35	grams	g
lb	pounds	0.454	kilograms	kg
T	short tons (2000 lb)	0.907	megagrams (or "metric ton")	Mg (or "t")
TEMPERATURE (exact degrees)				
°F	Fahrenheit	5 (F-32)/9 or (F-32)/1.8	Celsius	°C
ILLUMINATION				
fc	foot-candles	10.76	lux	lx
fl	foot-Lamberts	3.426	candela/m ²	cd/m ²
FORCE and PRESSURE or STRESS				
lbf	poundforce	4.45	newtons	N
lbf/in ²	poundforce per square inch	6.89	kilopascals	kPa
APPROXIMATE CONVERSIONS FROM SI UNITS				
Symbol	When You Know	Multiply By	To Find	Symbol
LENGTH				
mm	millimeters	0.039	inches	in
m	meters	3.28	feet	ft
m	meters	1.09	yards	yd
km	kilometers	0.621	miles	mi
AREA				
mm ²	square millimeters	0.0016	square inches	in ²
m ²	square meters	10.764	square feet	ft ²
m ²	square meters	1.195	square yards	yd ²
ha	hectares	2.47	acres	ac
km ²	square kilometers	0.386	square miles	mi ²
VOLUME				
mL	milliliters	0.034	fluid ounces	fl oz
L	liters	0.264	gallons	gal
m ³	cubic meters	35.314	cubic feet	ft ³
m ³	cubic meters	1.307	cubic yards	yd ³
MASS				
g	grams	0.035	ounces	oz
kg	kilograms	2.202	pounds	lb
Mg (or "t")	megagrams (or "metric ton")	1.103	short tons (2000 lb)	T
TEMPERATURE (exact degrees)				
°C	Celsius	1.8C+32	Fahrenheit	°F
ILLUMINATION				
lx	lux	0.0929	foot-candles	fc
cd/m ²	candela/m ²	0.2919	foot-Lamberts	fl
FORCE and PRESSURE or STRESS				
N	newtons	0.225	poundforce	lbf
kPa	kilopascals	0.145	poundforce per square inch	lbf/in ²

TABLE OF CONTENTS

LIST OF FIGURES	VI
LIST OF TABLES	VIII
ACRONYMS, ABBREVIATIONS, AND SYMBOLS	IX
EXECUTIVE SUMMARY	X
IMPLEMENTATION STATEMENT	XI
1. INTRODUCTION	1
2. OBJECTIVES	3
3. SCOPE	4
4. METHODOLOGY	5
4.1. Description of Failures Sites	5
4.1.1. Texas Test Sites	5
4.1.2. Louisiana Test Sites	7
4.2. Soil Characterization Tests	10
4.2.1. Grain Size Distribution	10
4.2.2. Atterberg Limit Tests	12
4.2.3. Standard Proctor Compaction Test	13
4.3. Unsaturated Soil Properties	14
4.3.1. Soil Water Retention Curve	14
4.3.2. Tempe Cell Apparatus	14
4.3.3. Dew Point Potentiometer	15
4.3.4. Test Procedure	16
4.3.5. Predicting Unsaturated Hydraulic Conductivity	16
4.4. Fully Softened Shear Strength	17
5. FINDINGS	21
5.1. Case History Database and Rehabilitation Techniques	21
5.2. Soil Water Retention Curves	22

5.3. Fully Softened Strength and Correlations.....	26
5.4. Climate Coupled Modeling of Highway Embankments.....	29
5.5. Framework for Evaluating Stability of Highway Embankment Slopes.....	30
6. CONCLUSIONS.....	32
7. RECOMMENDATIONS.....	33
REFERENCES.....	34

LIST OF FIGURES

Figure 1. Overview of Site 1 and photos of slope failure at Grayson County, Denison, Texas: (a) and (b) Denison Site overview and (c) tension cracks in the upper side of the slope.	6
Figure 2. (a) Aerial of Site 2, (b) damage at guard rails, and (c) tension cracks along slope surface.	7
Figure 3. Location of Louisiana Site 1: (a) aerial view of site, (b) failed embankments along highway, and (c) illustration of previous and current failure locations.	8
Figure 4. (a) Aerial of Louisiana failure Site 2, (b) location of slope failures, (c) desiccation cracks, and (c) scarp along roadway.	9
Figure 5. (a) Location of Site 3 in Louisiana, (b) photo of failed embankment, (c) rehabilitated failure with asphalt, and (d) failure scarp.	10
Figure 6. Grain size distribution of Texas Site 1.	11
Figure 7. Grain size distribution of Texas Site 2.	11
Figure 8. Grain size distribution of Texas Site 3.	12
Figure 9. Plasticity chart of Texas and Louisiana test sites.	13
Figure 10. Tempe cell apparatus.	15
Figure 11. Dew point potentiometer device.	15
Figure 12. Saturation of specimen.	16
Figure 13. Components of the ring shear device test setup.	18
Figure 14. Consolidation of I-10 sample for 100 kPa normal stress (red circles denote added soils and the orange dashed lines signify applied normal stresses).	19
Figure 15. Drained fully softened friction angle correlation for clay-size fraction (CF) > 20% (12).	20
Figure 16. SWRC of Texas Site 1 soil using the Van Genuchten (8) model.	23
Figure 17. SWRC of Texas Site 2 soil using the Van Genuchten (8) model.	23
Figure 18. SWRC of Texas Site 3 soil using the Van Genuchten (8) model.	24
Figure 19. SWRC of Louisiana Site 1 soil using the Van Genuchten (8) model.	25

Figure 20. SWRC of Louisiana Site 2 soil using the Van Genuchten (8) model.	25
Figure 21. SWRC of Louisiana Site 3 soil using the Van Genuchten (8) model.	26
Figure 22. FSS correlation envelopes for Texas sites.....	27
Figure 23. Ring shear test displacement and shear stress for Texas Site 1.....	27
Figure 24. Fully softened shear strength envelope for Texas Site 1.....	28
Figure 25. Ring shear test displacement and shear stress for Louisiana (a) I-10 and (b) I-55 sites.	28
Figure 26. Fully softened shear strength envelope for Louisiana (top) I-10 and (bottom) I-55 sites.	29
Figure 27. Climatic data obtained from the Louisiana State University Agriculimatic Data System.....	30
Figure 28. Elevated phreatic surface location in climate coupled model.	30

LIST OF TABLES

Table 1. Embankment failure risk classification system (2).....	2
Table 2. Summary of grain size distribution of Texas sites.....	12
Table 3. Summary of Atterberg limit test results.....	13
Table 4. Summary of standard compaction test results.	13
Table 5. Representative slope failures in Texas.....	21
Table 6. Embankment failure risk classification system (2).....	31

ACRONYMS, ABBREVIATIONS, AND SYMBOLS

CF	Clay size Fraction
CH	High Plasticity Clay
CL	Low Plasticity Clay
FSS	Fully Softened Strength
LADOTD	Louisiana Department of Transportation and Development
LSU	Louisiana State University
LTRC	Louisiana Transportation Research Center
MDD	Maximum Dry Density
OMC	Optimum Moisture Content
SWRC	Soil Water Retention Curve
TxDOT	Texas Department of Transportation
UTA	University of Texas at Arlington

EXECUTIVE SUMMARY

The purpose of this research is to build a framework to identify the high-risk slope by performing inverse stability analyses by using the determined soil properties at the laboratory to evaluate possible pore-water pressure and fully softened strength (FSS) that could have triggered the slope failures. The project consisted of six primary research phases. The first phase involves systematic review of documented embankment failures in Region 6 and evaluation of existing rehabilitation methods, which will be a methodology to determine the time to mobilize FSS and service life of highway embankments. Second phase involves conducting of FSS laboratory test of Louisiana and Texas soils. This laboratory test will be compared to empirical correlations to confirm if the correlation is applicable to the soils present at the project site, which can be used for design analyses. Further, the third phase involves finding unsaturated soil properties of the Louisiana and Texas soils through laboratory test. This test is conducted to evaluate the unsaturated hydraulic characteristics of failed embankment slope soils to predict the soil suction profiles by determining soil water retention curves (SWRC). SWRC helps to determine the depth of the moisture fluctuation, which in turn expects to identify the zone where the shear strength of clay will be varied due to the cycles of wetting and drying. SWRC tests are conducted and unsaturated hydraulic conductivity properties are determined to assess potential of soils for undergoing moisture intrusion and softening and this information will be used in the framework development. Fourth phase involves performing inverse stability analyses of documented failures. A slope failure indicates the factor of safety is unity along the observed sliding surface. The inverse analyses can be used to determine a previously unknown parameter, e.g. pore-water pressure or mobilized soil strength. In summary, this phase involves inverse analyses of failed embankments to link in situ pore-water pressure to environmental conditions (rainfall intensity and duration, drought, vegetation, etc.). Fifth phase involves developing a framework that predicts which locations have a high risks of slope failure in Region 6 and assess the reliability of the proposed model with field verification from documented slope failures. The probability of failure of a highway embankment is a function of the (1) moisture intrusion in the soil as related to soil suction, (2) time-dependent shear strength loss to FSS, and (3) slope inclination and soil properties. The outcomes of the previous phases are combined to develop a framework for predicting high-risk zones. The final phase involves determining cost-effective methods to repair landslides. There are several methods to mitigate the slope failure, including stabilized layers to plastic pins. This information will be compiled to provide a comprehensive list along with their constructability and cost related qualitative information, which could lead to a follow up research study which may require instrumented slopes on one or two select treatment methods and the performance of slopes over a period of time.

IMPLEMENTATION STATEMENT

The implementation of this research involves meetings with stakeholders, industry, and technical publications and presentations. The information provided in the implementation phase includes methods for estimating FSS and performing stability analyses of highway embankments. The specific outreach activities include the following:

1. **Technical Dissemination:** The research findings will be disseminated via journal publications and presentations. Relevant journals that the authors will submit include the ASCE Journal of Geotechnical and Geo-environmental Engineering, ASCE Journal of Materials in Civil Engineering, and Elsevier Transportation Geotechnics. Results were presented at the Tran-SET annual conference, along with national (ASCE Geo-Institute) and regional conferences. In particular, regional ASCE and Geo-Institute conferences are an important mechanism for connecting with industry practitioners. For example, the research results were presented at the 2018 Louisiana Transportation Conference. The results will be presented at the next Louisiana Civil Engineering Conference.
2. **National Technical Committees:** The researchers are members of the Geo-Institute Embankment, Dams, and Slopes (EDS) Technical Committee. The EDS committee has a subgroup that is writing a white paper on fully softened strength of high plasticity soils. The outcome of this research is assisting this subcommittee to write the state-of-practice in measuring drained shear strength, validating empirical correlations, and creating case histories for practical implementation. Similar input is provided to the TRB committee AFS10 Standing Committee on Transportation Earthworks.
3. **State DOTs:** The researchers held meetings and communicated with the Louisiana Department of Transportation and Development (LADOTD) and Texas Department of Transportation (TxDOT) engineers. These meetings provided updates to the research and facilitated research sites for testing. Next steps include discussing best practices for including the research results in highway embankment design/construction procedures.

1. INTRODUCTION

Each year, significant number of highway slope failures are reported all around the USA, especially from the regions where the native soil mostly consists of high plasticity clays. The preservation and resiliency of transportation infrastructure is extremely crucial for economic growth of the region and restoring daily mobility services. Many highway embankment slope failures are reported in the states of Texas and Louisiana, which results in constrained mobility services, high maintenance costs, and expensive rehabilitation costs. Initial research attributed these failures due to the presence of high plasticity clays that undergo significant volumetric changes from seasonal climatic fluctuation. Moreover, it was identified that weathering cycles (i.e., wetting-drying) resulted in desiccation cracks, which exposed the embankment fill material to increased moisture from precipitation. With increased moisture and softening of the soil, the shear strength reduced from a peak strength to fully softened strength. Because of the significantly lower strengths, frequent slope failures occur after rain events. More importantly, the frequency of such highway slope failures is predicted to increase in the future as the weathering conditions are impacted by higher rainfall intensities and longer durations of drought-like conditions. Considering these conditions, there is an urgent and important need (a) to develop a predictive tool for identifying such a high-risk location and (b) to determine cost-effective remedial methods.

The aim of this research is to develop the methodology and present findings for a predictive tool to identify high-risk slopes. To achieve this objective, medium to high plasticity soil samples were collected from slope failures from varying geological formations across the states of Texas and Louisiana. The research program included comprehensive laboratory tests such as physical index tests, shear strengths, and hydraulic properties. Further, inverse stability analyses were performed by using the laboratory soil properties to evaluate possible pore-water pressure conditions that could have triggered the slope failures.

Knowledge that Louisiana and Texas soils consist of significant amounts of high plasticity clay unsuitable for construction of highway embankments has been known since at least the early 1900s, Matson (1). Nevertheless, it was not until Burns et al. (2) that Louisiana started to conduct studies to document and understand the embankment failure mechanisms. Burns et al. (2) conducted a comprehensive review of 242 embankments with a combined 122 miles of highway transects along I-10 and I-20 in Louisiana. In total, 99 slopes had failed within 8-15 years post-construction. Failure locations, volumes, slope angles, and geological and geotechnical properties from failed and non-failed slopes were measured. The I-20 corridor resides between the Mississippi and Ouachita rivers. Soils typically consist of natural levee and alluvial deposits of fine-grained sediments. The study area focused on the flood plain of the Ouachita River, which is characterized by red clay and silts potentially from the Ozark area and gray clays and silts transported from the Ouachita Mountains. The I-10 corridor was characterized primarily by Prairie Terrace alluvium. The Calcasieu River, Bayou Lacassine, Mermentau Bayou, and the Vermillion River deposit modern alluvium in the study site. Soils in the I-10 region were characterized as being poorly to moderately drained and at moderate to high risk of shrinking and swelling. The researchers developed a risk classification framework (Table 1) which can easily be determined in a laboratory using Atterberg limits. While this

report was archived at Louisiana Transportation Research Center (LTRC), discussion with LADOTD engineers suggested the results were of this study were not incorporated into design.

Table 1. Embankment failure risk classification system (2).

Risk Level	Clay Content (%)	Plasticity Index	Liquid Limit	Net Smectite	Chance Of Failure
High	>47	>29	>54	>33	85-90
Intermediate	32-47	16-29	36-54	18-33	55-60
Low	<32	<16	<36	<18	<5

The findings of Burns et al. (2) were digitized into a database and distributed to LADOTD Headquarters, who encouraged their geotechnical engineers to populate the database with any known failures which were missing. The database was also updated with observed failures along the I-10 and I-12 corridors. The product of the accumulated database will be a large dataset of embankment failures in Louisiana and characteristics.

2. OBJECTIVES

The main objectives of this study are (a) to develop a framework that can predict the locations which have a high risk of slope failure and demonstrate its applicability in Region 6, and (b) to identify cost-effective rehabilitation techniques for repairing slides. To accomplish the proposed objectives, the following research tasks were conducted:

- Task 1 systematically reviews documented embankment failures in Region 6 and evaluates existing rehabilitation methods. A methodology to determine the time to mobilize FSS and estimate service life of highway embankments is developed.
- Task 2 involves laboratory testing of fully softened strength (FSS) of Louisiana and Texas soils. The obtained laboratory test results are compared with that estimated using empirical correlations to confirm if the correlations are applicable to the soils present at the project site, which are being used for design analyses.
- Task 3 involves laboratory testing of unsaturated soil properties of Louisiana and Texas soils. This test evaluates the unsaturated hydraulic characteristics of failed embankment slope soils to predict the soil suction profiles by determining SWRC. SWRC helps to determine the depth of the moisture fluctuation, which helps to identify the zone where the shear strength of clay varies due to the cycles of wetting and drying. SWRC tests are conducted and unsaturated hydraulic conductivity properties are determined to assess potential of soils for undergoing moisture intrusion and softening. This information is utilized in the framework development in Task 5.
- Task 4 involves inverse stability analyses of documented failures. A slope failure indicates the factor of safety is unity along the observed sliding surface. The inverse analyses are used to determine a previously unknown parameter, e.g. pore-water pressure or mobilized soil strength. In summary, Task 4 involves inverse analyses of failed embankments to evaluate the in-situ pore-water pressure based on environmental conditions (rainfall intensity and duration, drought, vegetation, etc.).
- Task 5 involves developing a framework that predicts which locations have a high risks of slope failure in Region 6 and assess the reliability of the proposed model with field verification from documented slope failures. The probability of failure of a highway embankment is a function of the (1) moisture intrusion in the soil as related to soil suction, (2) time-dependent shear strength loss to FSS, and (3) slope inclination and soil properties. The outcomes of Tasks 1 to 4 are combined to develop a framework for predicting high-risk zones.
- Task 6 involves determining cost-effective methods to repair landslides. There are several methods to mitigate the slope failure, including stabilizing layers to plastic pins. This information provides a comprehensive list along with their constructability and cost related qualitative information, which leads to a follow up research study which may require instrumented slopes on one or two select treatment methods and the performance of slopes over a period.

3. SCOPE

The purpose of this research is to find the methodology for developing a predictive tool to identify the high-risk slopes. For which three slope failure test sites in Texas and three test sites in Louisiana were identified and samples were taken from the failure scarp to conduct tests including Atterberg limits (plastic limit and liquid limit), clay size fraction (CF), standard Proctor compaction test, FSS, and SWRC tests. Amongst the various causes for the slope failure, this study is limited to determine FSS and evaluate possible pore-water pressure that could have triggered the slope failures.

4. METHODOLOGY

The presented research study targets to determine the slopes which are under high risk of failure and test its validity in Region 6 and provide the cost-effective rehabilitation methods. To achieve the main objective of the study, a systematic literature review was performed on the documented slope failures in Region 6 to understand the climatic and meteorological events during the service life, time required to mobilize FSS, and performance of rehabilitation methods. Six (6) slope failures with three (3) in Texas and Louisiana were identified and described herein. Samples were taken from the slope failure scarp to conduct basic and advanced laboratory tests. To determine basic soil properties, Atterberg limit, grain size distribution, clay size fraction, and standard proctor compaction tests were conducted in accordance with related ASTM standards. The basic soil properties test results are listed and soils are classified based on the Unified Soil Classification System (USCS). The laboratory test program was mainly designed to determine the softening of the soil due to wetting and drying cycles and unsaturated hydraulic conductivity properties. The FSS test gives the long-term soil strength and was conducted with the Bromhead Ring Shear Apparatus according to the modified procedure described by Stark and Eid (3). SWRC test provides the unsaturated behavior of the soil and this test was conducted with Tempe cell and Dew Potentiometer Apparatus. The site descriptions and the methodologies of basic and advanced material characterization tests for soils are provided in the following sections.

4.1. Description of Failures Sites

4.1.1. Texas Test Sites

Texas Site 1 is located near Randell Lake, Denison, Texas along U.S 75 Frontage Road (Figure 1(a)). The embankment at this site has an approximate height of 30-35 feet. The site is overlain by the deposit of Fort Worth Limestone as per geological formation. This site experienced severe desiccation cracks starting in 2014, which resulted in a major slope failure in 2016 and caused extensive damage to the overlying pavement that lead to the closure of road. The soil sample was collected from the south side of the embankment where it had several failures and desiccation cracks from the failure scarp from a depth of approximately one foot below the surface, as the surface was covered by soil vegetation. Figures 1(b) and 1(c) show the major cracks in the upper side of the slope and there are significant number of desiccation cracks and several shallow slope failures along the embankment.

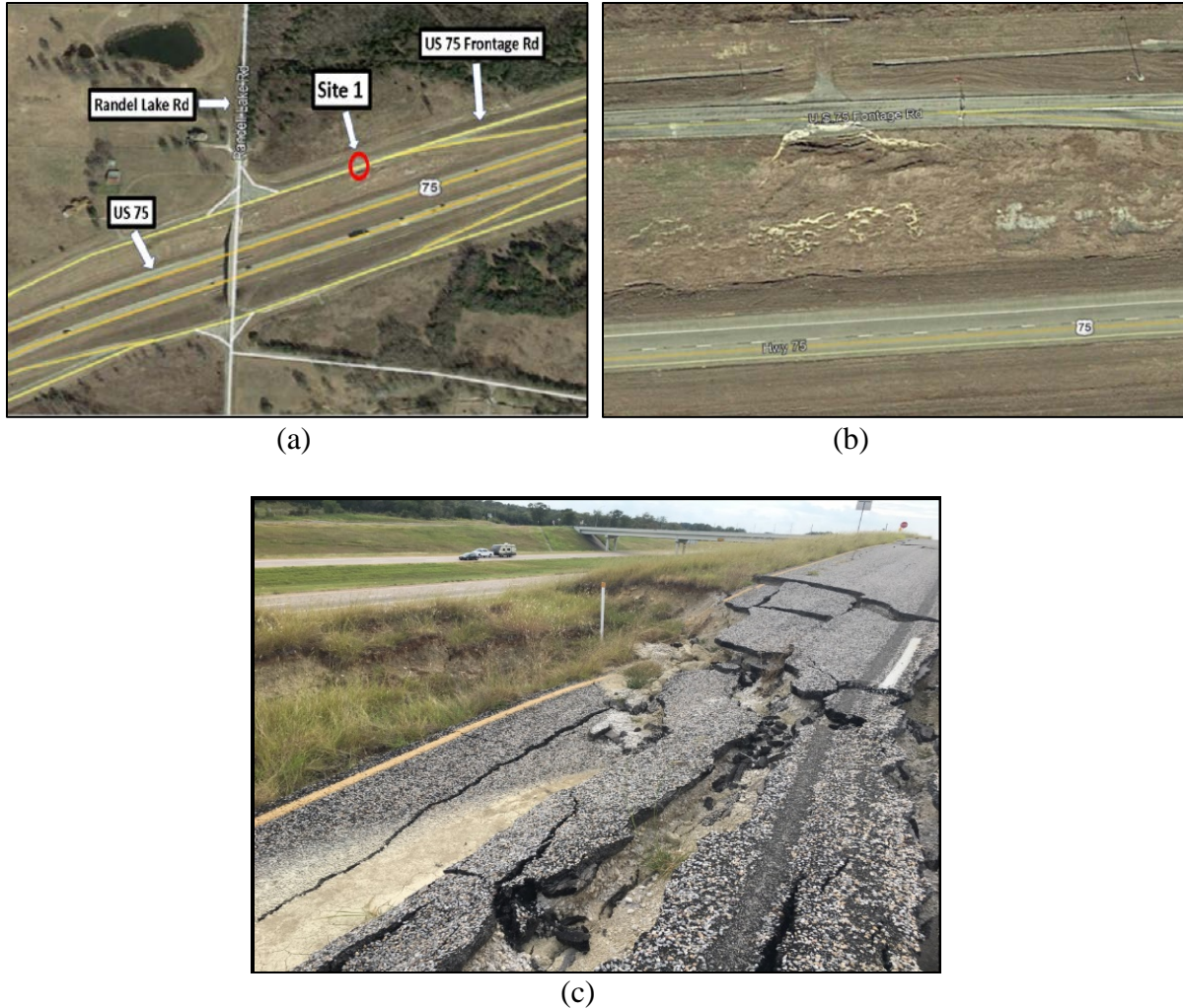


Figure 1. Overview of Site 1 and photos of slope failure at Grayson County, Denison, Texas: (a) and (b) Denison Site overview and (c) tension cracks in the upper side of the slope.

Sites 2 and 3 are located over Highway 82 in Paris, Texas. Site 2 is located near the intersection of FM79 and Site 3 is located nearby N Main Street. According to TxDOT employees, Sites 2 and 3 frequently incurred failures. The embankment slope at Site 2 experienced recurring slope failures, specifically at the crown of the slope, damaging guardrails and shoulder of highway (Figure 2(b)). A significant number of deep desiccation cracks was noticed along the highway embankment. In Site 2, the sample was collected one foot below the ground surface from the south side of the embankment near the slope failure. Additives were used in the soil for stabilization which was recognized when collecting the samples. The slope failure at Site 3 was repaired several times by pushing the same material back into place, with the last failure occurring in 2015. The soil samples were collected from the south side of the embankment, 1 foot below the surface.



(a)



(b)



(c)

Figure 2. (a) Aerial of Site 2, (b) damage at guard rails, and (c) tension cracks along slope surface.

4.1.2. Louisiana Test Sites

Louisiana Site 1 is located along I-55 near Hammond, Louisiana (Figure 3(a)). The site was chosen in cooperation with LADOTD headquarters after discussion with district engineers. The site features a highway overpassing a railroad. Drainage holes in the bridge were plugged to stop settlement of the under passing rail line. Four embankments at this site previously failed, specifically each of the abutments failed following the bridge drainage holes being plugged with cement. Three of the four failed embankments were repaired using deep-soil mixing (locations 1, 2, and 3 in Figure 3(c)), and the bridge abutments are currently being repaired using a soil-nail wall. The fourth failed embankment is being closely monitored and will be used as a test-embankment in cooperation with LADOTD District 62 engineers. Soil samples were taken from the failure scarp and brought back to Louisiana State University (LSU) for testing. Soil borings taken for the previous embankment failures show stiff, high plasticity clays to a depth of 120 feet below the ground surface. Some very stiff lean clays (CL) are interbedded in some cores, but the stratigraphy is dominated by tan and gray high plasticity clays (CH).



(a) (b)



(c)

Figure 3. Location of Louisiana Site 1: (a) aerial view of site, (b) failed embankments along highway, and (c) illustration of previous and current failure locations.

Site 2 is located approximately 30 km southwest of Natchitoches, Louisiana (Figure 4(a)) and is situated in close proximity to the Red River. The site features a roadway sitting on top of a levee separating local communities from Nantachie Lake (Figure 4(b)). The site experienced multiple failures which led to the roadway being closed by the LADOTD Dam Safety division (Figure 4(d)), though locals still drive around the barriers. Extensive desiccation cracking was

observed along the failure scarps as well as in the embankment sections which had not yet failed, measuring to an average of approximately 45 cm (Figure 4(c)).

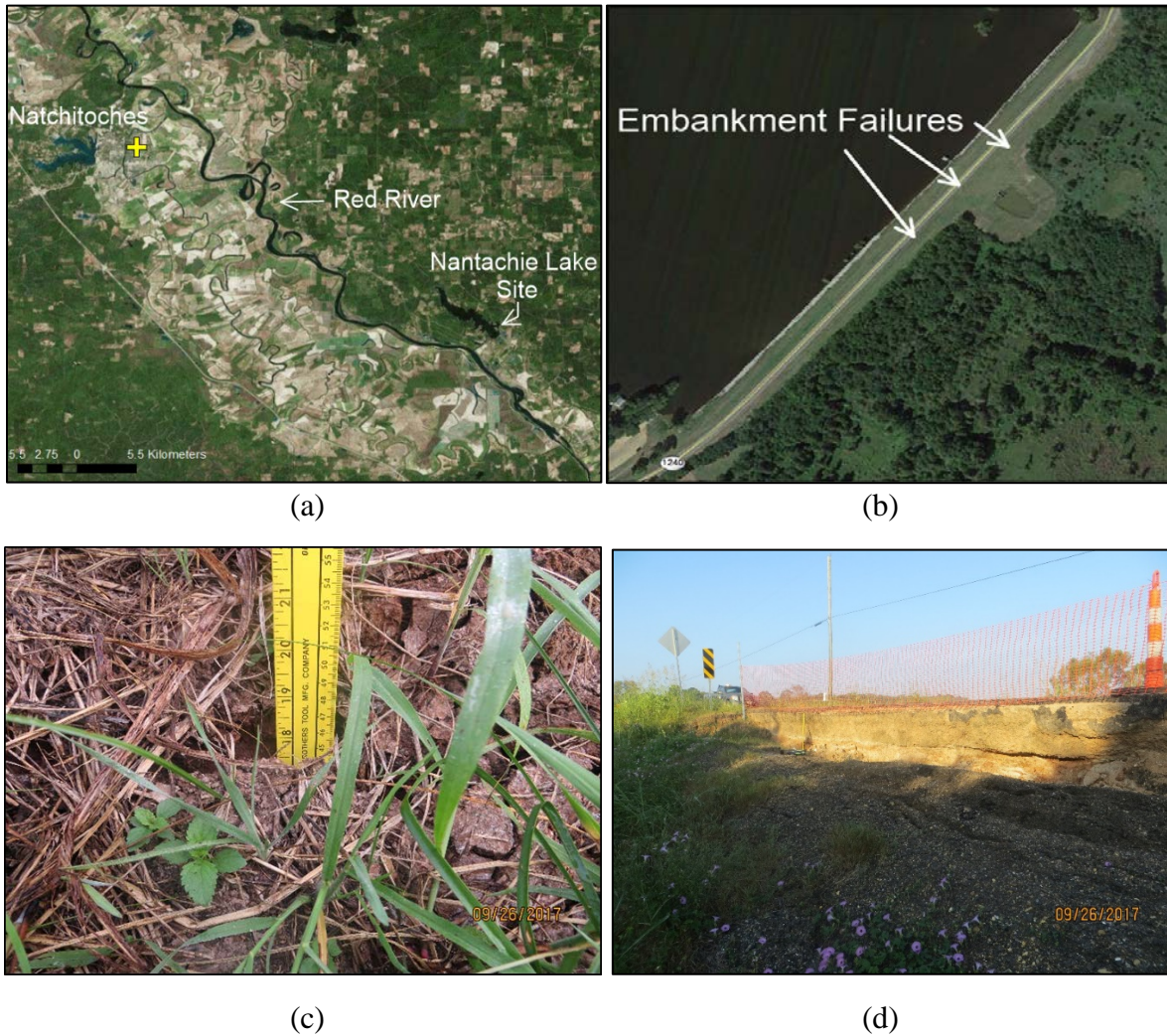


Figure 4. (a) Aerial of Louisiana failure Site 2, (b) location of slope failures, (c) desiccation cracks, and (c) scarp along roadway.

Site 3 is located along I-10 at Welsh, Louisiana (Figure 5(a)). The site is geologically characterized by the Pleistocene terrace deposits, in which Burns et al. (2) found significantly fewer failures. Failures in the adjacent embankments were likely excavated and filled with asphalt materials (Figure 5c). A longitudinal scarp was observed at the site. Soils taken from Site 3 were similar in characterization to the soils taken from Site 1.

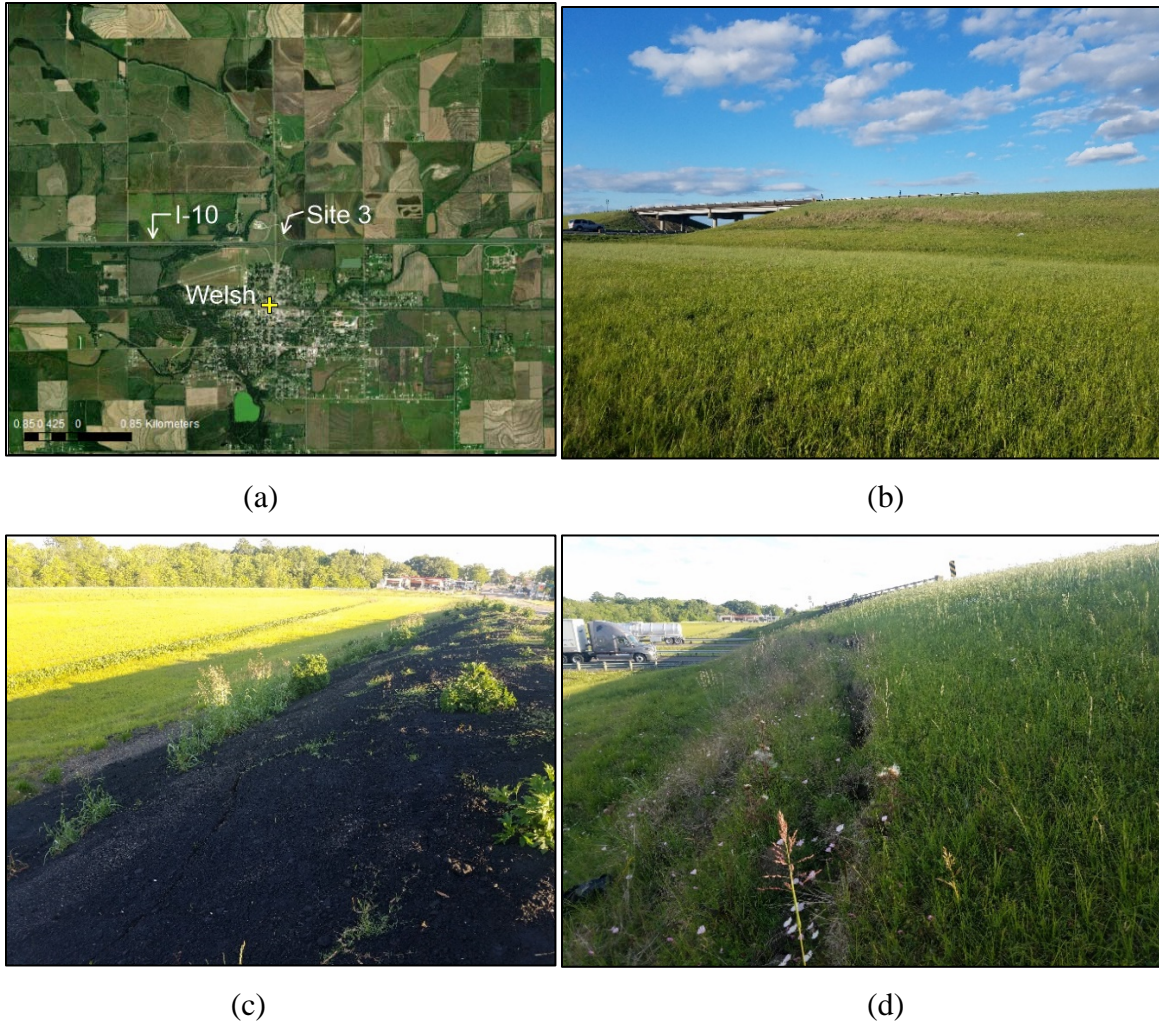


Figure 5. (a) Location of Site 3 in Louisiana, (b) photo of failed embankment, (c) rehabilitated failure with asphalt, and (d) failure scarp.

4.2. Soil Characterization Tests

Towards determining the physical characteristics of the soil collected from the six sites, an experimental program was conducted to obtain Atterberg limits, clay size fraction, FSS, and SWRC tests.

4.2.1. Grain Size Distribution

Wet Sieve analyses were conducted on samples to determine the grain size distribution following the procedure of ASTM D422-63. The soil was first dried in an oven at the temperature of 120° to 140°F. After drying, the soil was crushed and washed using No. 200 sieve. The soils retained on No. 200 sieve were dried in oven and were sieved through US standard sieves including number 4, 10, 30, 40, 60, 100 and 200. The weights of soil in each sieve was measured and the distribution of grain size larger than 74 μm was determined in this method. Finally, a hydrometer test as per ASTM D422-63 was conducted on soils passing the

No. 40 sieve. By using both wet sieve and hydrometer tests, the grain size distribution curves were developed as shown in Figures 6, 7, and 8.

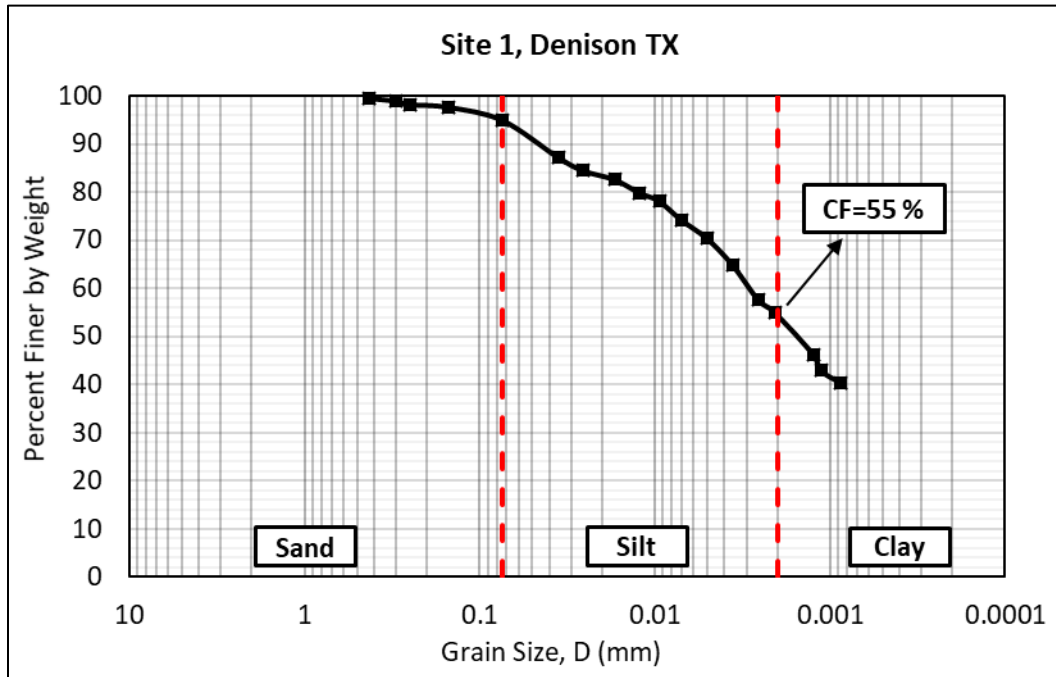


Figure 6. Grain size distribution of Texas Site 1.

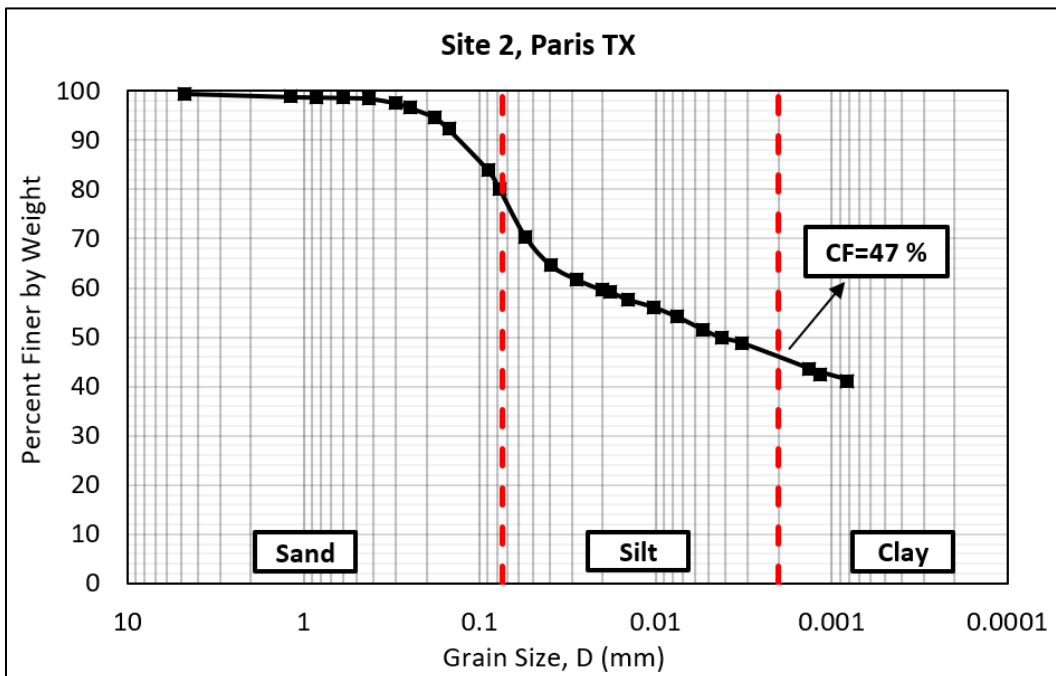


Figure 7. Grain size distribution of Texas Site 2.

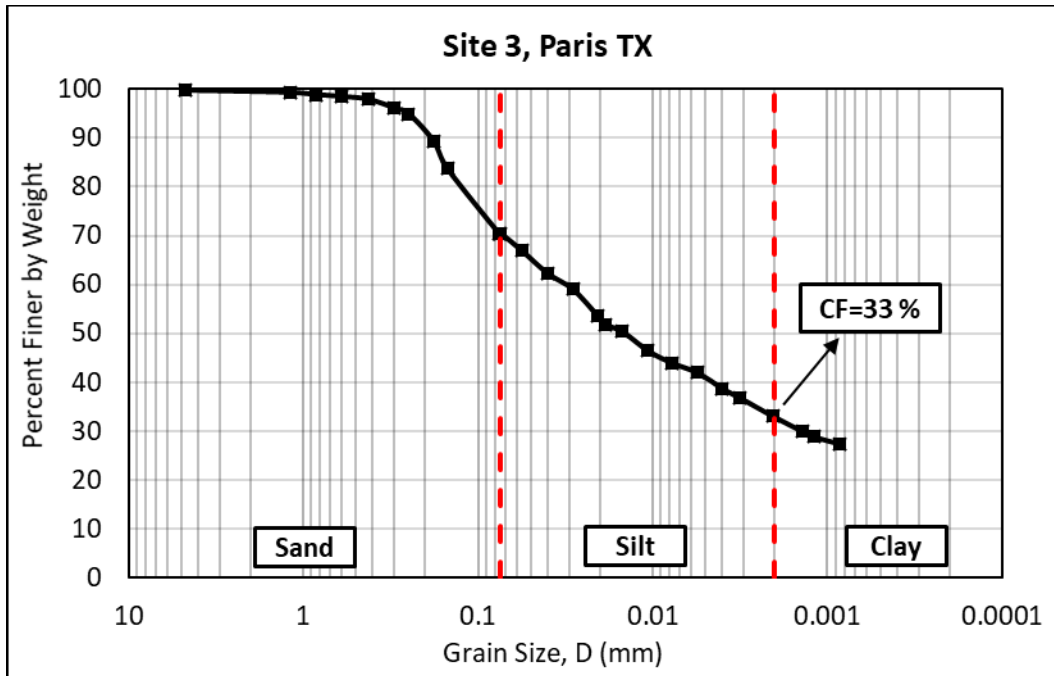


Figure 8. Grain size distribution of Texas Site 3.

The particle size distributions for the Texas sites indicate that the highest clay size fraction of 55% is at Site 1. Site 2 contains 47% clay size fraction, while Site 3 contains the lowest clay size fraction of 33%. The summary of grain size distribution of Texas sites is listed in Table 2.

Table 2. Summary of grain size distribution of Texas sites.

Test Site	Sand (%)	Silt (%)	Clay (%)
Site 1	5	40	55
Site 2	20.5	32.5	47
Site 3	28.8	38.2	33

4.2.2. Atterberg Limit Tests

Atterberg limit tests were performed to identify the basic properties of soil collected from the six sites according to techniques outlined in ASTM D 4318. By adding water to soil, soil state initially transforms from dry to semi-solid form then to plastic form and finally to liquid stage. For Texas sites, laboratory tests showed that the Liquid Limit (LL) and Plastic Limit (PL) values ranged from 43 to 61 and 21 to 27, respectively. Site 1 contains the highest plasticity index (PI) with 37, while Site 3 has the lowest PI with 26. The Atterberg limit test results including plasticity index and liquid limit for the soils from Texas and Louisiana sites are presented in Figure 9. Table 3 lists the Atterberg limits for Louisiana and Texas sites.

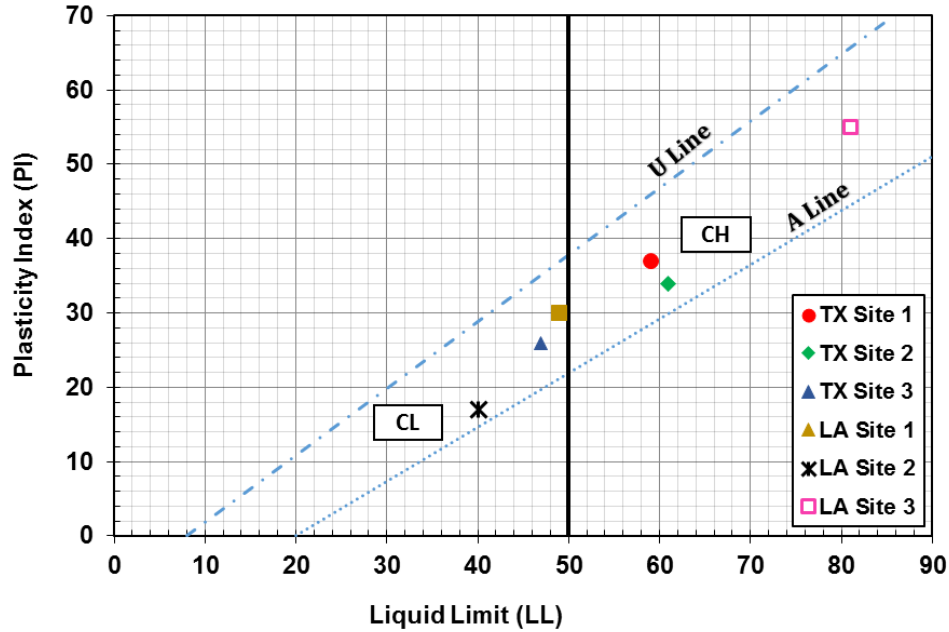


Figure 9. Plasticity chart of Texas and Louisiana test sites.

Table 3. Summary of Atterberg limit test results.

Test Site	Liquid Limit	Plastic Limit	Plasticity Index	USCS Classification
TX Site 1	59	22	37	CH
TX Site 2	61	27	34	CH
TX Site 3	47	21	26	CL
LA Site 1	49	19	30	CL
LA Site 2	40	23	17	CL
LA Site 3	81	26	55	CH

4.2.3. Standard Proctor Compaction Test

Standard compaction tests were conducted by following the procedure of ASTM D698-12. This test gives the relationship between soil water content and dry unit weight. The peak point of the compaction curve provides the optimum moisture content (OMC) of the soil and the corresponding maximum unit weight (or maximum dry density). After the oven drying process, the Maximum Dry Density (MDD) value is calculated. Samples for SWRC tests are prepared and tested at 95% MDD condition. Table 4 presents the MDD and OMC for the soils from Texas test sites.

Table 4. Summary of standard compaction test results.

Test Site	Maximum Dry Density (pcf)	Optimum Moisture Content (%)
TX Site 1	108	20
TX Site 2	98	22.5
TX Site 3	105	19
LA Site 1	104	18
LA Site 2	107	14
LA Site 3	105	17

4.3. Unsaturated Soil Properties

During the drought season, the degree of saturation of the embankment soil drops substantially leading to changes in the hydraulic conductivity. Darcy's law is used to determine the saturated hydraulic conductivity. However, unsaturated hydraulic conductivity is not a constant value because it varies with soil matric suction. For example, an increase in soil matric suction level decreases unsaturated soil hydraulic conductivity. Fredlund and Rahardjo (4) stated that during rainy season, desiccated soils with higher permeabilities will increase rain infiltration into slopes causing an increase in pore-water pressures in the zone above the groundwater table. In addition, the groundwater table may rise to result in a further increase in pore-water pressures. As a result, the shear strength of the soil will decrease and factor of safety of the slope can drop below a critical value, triggering slope failure. Hence, SWRC tests for the soils were conducted to predict the infiltration and pore-water pressure increase in the embankments.

4.3.1. Soil Water Retention Curve

SWRC depends on the soil type, grain size distribution, density, and temperature. Fredlund (5) describes the entire the SWRC using three zones: (1) boundary effect zone, (2) transition zone, and (3) residual zone. Boundary effect zone indicates negligible change in water content with an increase in suction level. The transition zone is represented by a sudden decrease in water content with corresponding increase in suction. The residual zone indicates minimal water content change with increase in suction level. These zones are separated by air-entry value and residual suction level. There are different laboratory test methods to measure the components of the total suction and matric suction to develop SWRC. For this study, Tempe cell apparatus and WP4C Dew Point Potentiometer apparatus were utilized. Tempe cell apparatus was used for relatively low suction range, i.e. from 0 to 10,442 psf (500 kPa) whereas the WP4C was used for high suction values.

4.3.2. Tempe Cell Apparatus

Tempe cell apparatus applies and maintains matric suction on the soil specimens by using the axis translation technique proposed by Hilf (6). The soil sample is placed on the HAE ceramic disk, and then the retaining cylinder is covered before applying the required air pressure (Figure 10). The test is started by applying a small air pressure (about five kPa) on a saturated soil specimen and the volume of water expelled from the specimen before reaching equilibrium is recorded. This generates the first point on the SWRC, and additional points are obtained by changing the applied air pressure in the Tempe cell. The air-water menisci present in the pores of the saturated ceramic disk prevents the air to pass through the disk but allows water from the soil specimen to flow through it. This phenomenon enables maintaining the desired air pressure and suction level required to perform the test. At the end of the test, the water content of the specimen at different applied suction levels is back-calculated based on the volume of water expelled from the specimen. In this research, a ceramic disk with an air entry value of 5

bars (500 kPa) was used. To determine the remaining portion of the SWRC corresponding to relatively high suction range, the Dew Point Potentiometer apparatus was utilized.

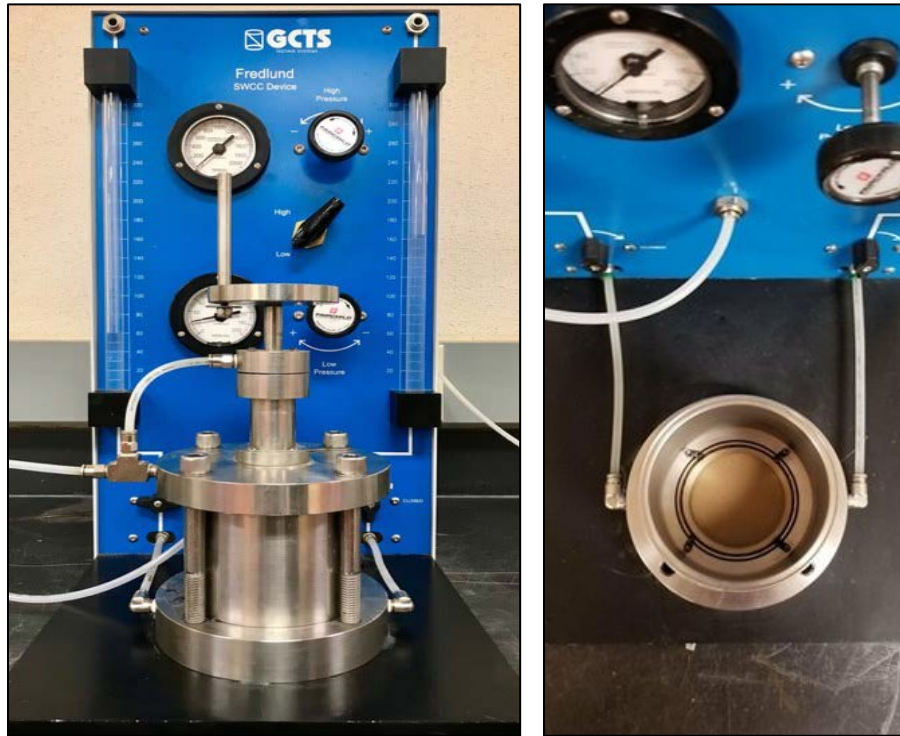


Figure 10. Tempe cell apparatus.

4.3.3. Dew Point Potentiometer

WP4C Dew Point Potentiometer determines the water presence for high suction range by determining the amount of the relative humidity above the soil. WP4C apparatus adopts the chilled-mirror technique as given in ASTM D6836. The soil sample is placed in the closed chamber that has a mirror, optical sensors, and temperature sensors. At equilibrium stage, the amount of relative humidity is in relationship with the soil suction level. Figure 11 shows the WP4C Dew Potentiometer apparatus used in this research study.



Figure 11. Dew point potentiometer device.

4.3.4. Test Procedure

The drying path of SWRC was obtained using Tempe cell and Dew Point Potentiometer. For less than 500 kPa suction value, Tempe cell apparatus was used. The required amount of air dried soil was pulverized and passed through the No. 40 sieve. The soil samples were prepared at a maximum dry density of 95% by using the OMC value obtained from standard compaction test. The samples were compacted under static compaction with 1.7 mm/ min compaction rate. To ensure the uniform distribution of moisture throughout the sample, they were kept in the humidity-controlled room for 48 hours. In Figure 12, specimens were confined in all the directions and were left submerged in the distilled water for at least 72 hours to obtain 100% degree of saturation. At the same time, the ceramic disk was saturated in Tempe cell at a pressure of 100 kPa for 24 hours. The SWRC was obtained by changing the air pressure while keeping the pore water pressure equal to the atmospheric pressure. Once the air pressure was applied in the cell, the water present in the pores was expelled from the specimen until the water and air phase reached an equilibrium. The matric suction was increased in steps and water content was calculated at every step by recording the amount of water leaving the sample.

For higher suction ranges, the WP4 apparatus was utilized. The soil samples were cut into a smaller size and placed in the chamber which was cleaned to prevent contact with soil samples and the relative humidity sensor. After locking the container, the presence of relative humidity above the soil was measured. When the relative humidity reaches the equilibrium, the potentiometer displays the total matric suction of the soil specimen. At each step, soil water content was measured and the SWRC plotted.

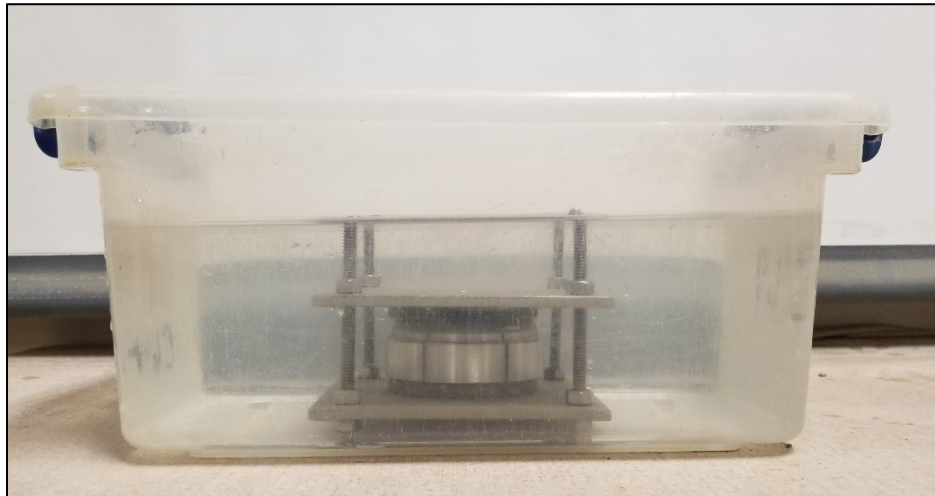


Figure 12. Saturation of specimen.

4.3.5. Predicting Unsaturated Hydraulic Conductivity

To predict the SWRC, many empirical equations are available (7,8,9). These equations can be divided into two and three constant fitting parameters and are utilized to fit the obtained SWRC data. In this research, the Van Genuchten (8) model was used, which uses three constant fitting parameters:

$$\theta = \frac{\theta - \theta_r}{\theta_s - \theta_r} = \left(\frac{1}{1 + (\alpha\psi)^n} \right)^m \quad [1]$$

where:

θ = volumetric water content,

θ_s = saturated water content,

θ_r = residual water content, and

α , n and m = constant soil parameters.

In the Van Genuchten (8) best fitting equation, α , n and m are related to inverse of air entry value of soil, soil pore size distribution, and symmetry of the curve, respectively. Soils with smaller particle sizes correspond to smaller n value, whereas soil with high air suction value corresponds to a smaller α value. The unsaturated hydraulic conductivity was obtained from the SWRC curves using the best fitting curve parameters from Van Genuchten model (8).

4.4. Fully Softened Shear Strength

To measure the fully softened shear strength, the modified Bromhead ring shear apparatus described by Stark and Eid (3) was used in accordance with ASTM (D7608-10) to determine FSS envelopes. The modified Bromhead ring shear apparatus uses an annular specimen with an inside diameter of 70 mm (2.75 in) and an outside diameter of 100 mm (4 in). The modified Bromhead ring shear testing procedure has been completed on the Louisiana soils and is approximately halfway finished on the Texas soils. The I-55 soil sample is from the Hammond, LA site, while the I-10 sample comes from exit 54 which contains 4 separate embankment failures at the overpass. The ring shear tests were performed at effective normal stresses of 12 kPa, 50 kPa, and 100 kPa. The sample preparation involves mixing the soil at 1.5 times the liquid limit, consolidated to the effective normal stress, and sheared at a rate of 0.018mm/min. Figure 13 shows the components of the ring shear device.



Figure 13. Components of the ring shear device test setup.

The consolidation phase of sample preparation is a time-consuming process. Each sample requires multiple series of adding additional soils as they consolidate at effective stresses. In particular, the 12 kPa normal stress does not need an additional consolidation stage. For the 50 kPa normal stress, the sample consolidates for about one hour at 12 kPa before the normal stress is raised to 50 kPa, where it consolidates for 2 hours. After the sample compresses, more soil is added to the container and the consolidation process restarts from 12 kPa. For the 100 kPa normal stress, additional soil is added at 50 kPa and then another two times at the 100 kPa. In other words, the consolidation process can last 2 to 3 days before the shearing phase is

started. Figure 14 shows an example of the consolidation process to 100 kPa, where the circles represent times when a load was applied to the soil. In this case, the consolidation stage lasted about 48 hours.

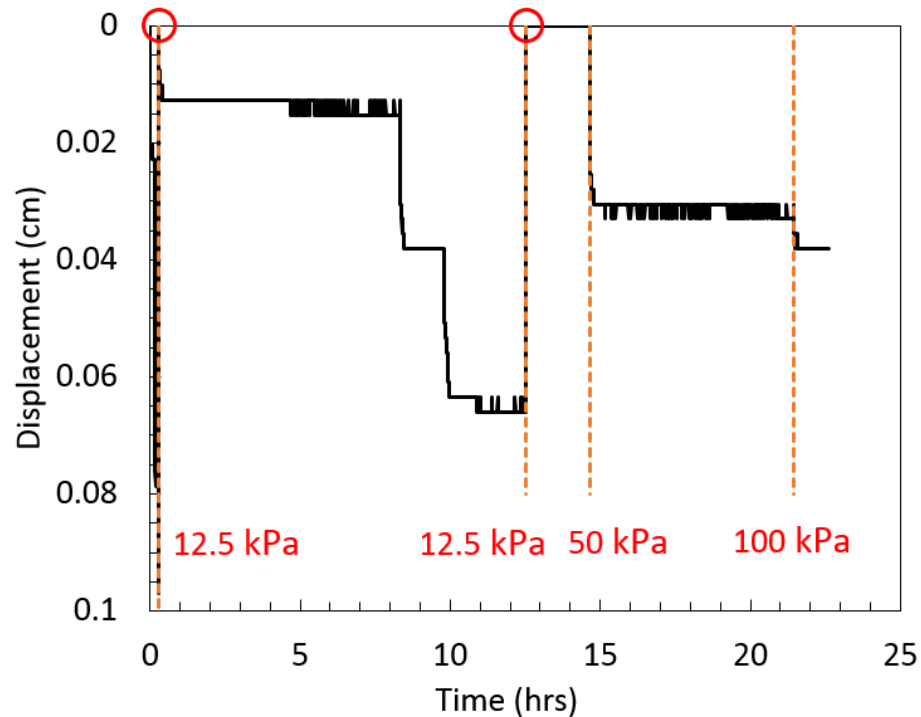


Figure 14. Consolidation of I-10 sample for 100 kPa normal stress (red circles denote added soils and the orange dashed lines signify applied normal stresses).

Three main correlations have been published to estimate the FSS envelope, Stark and Eid (3) augmented by Stark et al. (10), Stark and Hussain (11), and Gamez and Stark (12). The correlations estimate the effective normal stress-dependent FSS envelope using liquid limit, clay-size fraction, and plasticity index. Figure 15 shows the correlations from Gamez and Stark (12). To develop the non-linear strength envelop, the clay-size fraction (CF) and liquid limit (LL) are measured using the hydrometer and Atterberg cup, respectively. With these properties, the secant friction angle is evaluated for normal effective stresses of 12 kPa, 50 kPa, and 100 kPa. The non-linear shear strength is formed by using the secant friction angle and normal effective stress. For normally consolidated soils, the cohesion intercept is zero.

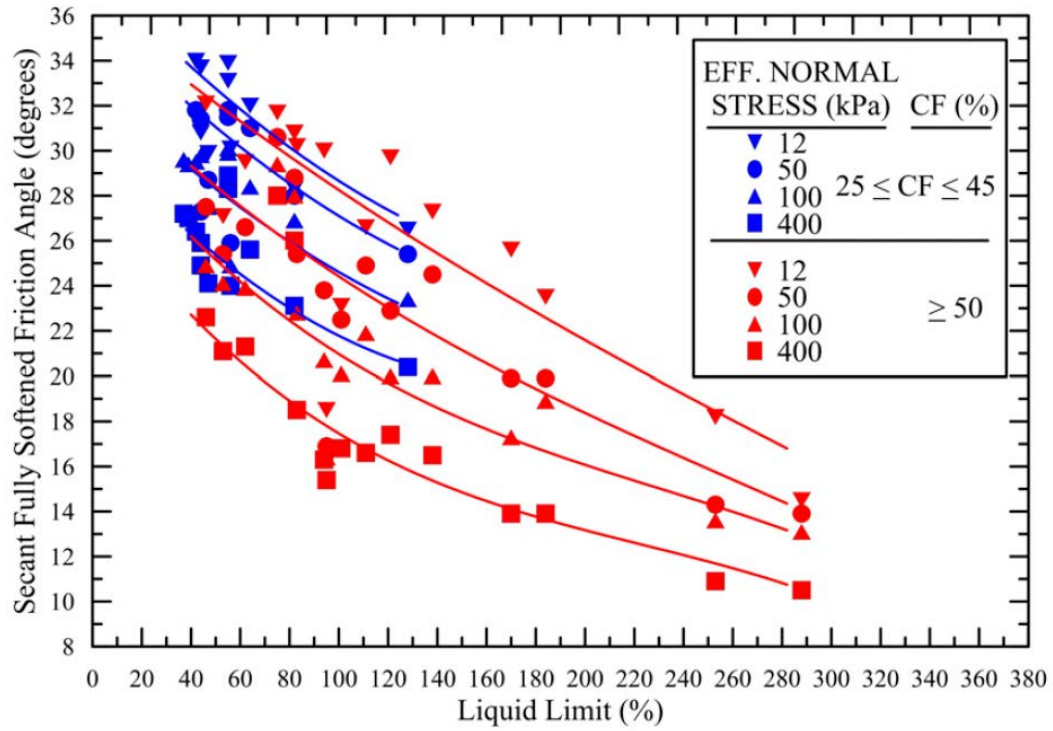


Figure 15. Drained fully softened friction angle correlation for clay-size fraction (CF) > 20% (12).

5. FINDINGS

5.1. Case History Database and Rehabilitation Techniques

The LSU researchers visited the LADOTD headquarters and local districts to survey and document the propensity of highway embankment failures across the state. It was immediately apparent that a formal procedure was not available to document the important facts of highway embankment failures, including failure date, embankment geometry, construction history, rehabilitation methods, index soil properties, and rehabilitation date. As a result, the collected data were obtained from informal survey of the geotechnical engineers based on recollections and reoccurring sites. The researchers compiled the available case histories and provided this information to LADOTD as an EXCEL spreadsheet. The columns were tabulated with relevant information that they can fill out with future failures.

The University of Texas at Arlington (UTA) team met with TxDOT engineers and visited several test sites where slope failures had occurred in the past. However, those case histories did not have detailed information on the exact failure dates, embankment geometries, material properties, and rehabilitation history. The UTA research team reviewed available literature and compiled some of the most notable slope failures that occurred in Texas which are presented in Table 5.

Table 5. Representative slope failures in Texas.

Number	Embankment Slope Location	Height of slope(ft)	Slope Ratio	Time of Failure
1	Tarrant County, Texas	36	2.5H:1V	October 2011
2	Fort Worth, Texas	20	3H:1V	February 2001
3	Midlothian, Texas	30	3H:1V	September 2010
4	Dallas, Texas	18	3H:1V	2009
5	Round Rock, Texas	21	3H:1V	1992, 1999, 2003

This paucity of case histories prevented the researchers to develop any broad conclusions of the time to failure. Anecdotal evidence suggests the service life of the embankments ranges from 20 to 30 years, with an average life span of 25 years. The overwhelming question posed throughout the discussions was how one area can fail while the immediate neighboring slope did not. Assuming the embankment soils are at fully softened strength, two possibilities are that the soil in the failed slope contains higher clay-size fraction and liquid limits (i.e., lower drained shear strength) and localized desiccation cracks provided conduits for the pore-pressure to increase such that a slough formed. The first mechanism is attributed to the spatial variability of soil properties within an embankment, which stems from LADOTD requiring a low plasticity soil (e.g., $PI < 20$) as construction specifications. More likely, the unsaturated soil hydraulic properties and desiccated cracks lead to some locations to fail before others. An outcome of this research is the need for field monitoring of highway embankments to understand the in-situ hydraulic conditions as a function of the Louisiana climate.

The lessons learned from the database also extends to the rehabilitation methods. In Louisiana, the overwhelming majority of embankments were repaired using the methodology outlined in Zhang et al. (13). In particular, the failed slope is excavated back to a stable bench. Soils with lower PI are typically used. Nonwoven geotextiles are placed at a 12-inch vertical spacing to provide a form of reinforcement. Discussions with LADOTD engineers indicate that while a failure using this solution has yet to be documented, it is not known if the service life of the

embankment is extended further than the average 25 years. In fact, many of the first cases are reaching this threshold and it will be important to track how these slopes perform moving forward. LADOTD also recently attempted a value engineering project through a contract with Hayward Baker, where cement grout vertical shear walls were constructed at a spacing. The value is using the in-situ soils and not needing to truck in lower PI soils. The research team also brought in Tencate Mirafi to discuss additional cost-effective techniques for slope rehabilitation. The Tencate engineers noted that the geotextiles recommended in the current methodology is hydrophobic. In other words, it does not provide any drainage capacity and is likely only providing some degree of reinforcement to limit deformations and subsequent failure. An alternative to the current geotextile is the H2Ri woven geotextile because it provides wicking capability, i.e., it actively removes water from the soil. The degree of water removal is a function of the soil type and in-situ matric suction, but it represents a technique that can limit the rise of pore-water pressure during an extreme precipitation event. In fact, the research team is working with Tencate on finding a project site to implement a field study to compare between the current method with the H2Ri geotextile. The LSU team identified the Hammond site along I-55 as a potential suitor. However, delays in the let date has pushed back the possibility of leveraging this Tran-SET project for practical application. Nevertheless, an outcome of this research project will likely be future collaboration with LSU and Tencate. The UTA team has extensive experience with repair of highway embankment slopes. They currently have collaboration with TxDOT to implement a repair that involves constructing a veneer of lime stabilized soil to prevent desiccation of the top soil and hence infiltration of rainfall into the slope.

5.2. Soil Water Retention Curves

SWRC was determined using the Tempe cell and Dew Point Potentiometer Apparatus. In this study, 95% MDD condition soil samples were subjected to SWRC tests. The changes of the volumetric water content and the corresponding suction levels of the soil samples were measured and SWRCs plotted. Experimentally obtained SWRCs are presented with the commonly used Van Genuchten (8) best fitting SWRC model.

Texas Site 1 soil has a 47.8% maximum saturated volumetric water content and 4.8% residual volumetric water content. The air entry value of Site 1 is 65 kPa (9.43 psi). For Site 1, the best fitting parameters obtained from Van Genuchten (8) model are $\alpha=0.01 \text{ kPa}^{-1}$, $n=2.89$, $m=0.095$.

Texas Site 2 soil has a 44.3% maximum saturated volumetric water content and 5.2% residual volumetric water content. The air entry value of Site 2 soil is 70 kPa (10.15 psi). For Site 2, the best fitting parameters obtained from Van Genuchten (8) model are $\alpha=0.008 \text{ kPa}^{-1}$, $n=1.54$, $m=0.165$.

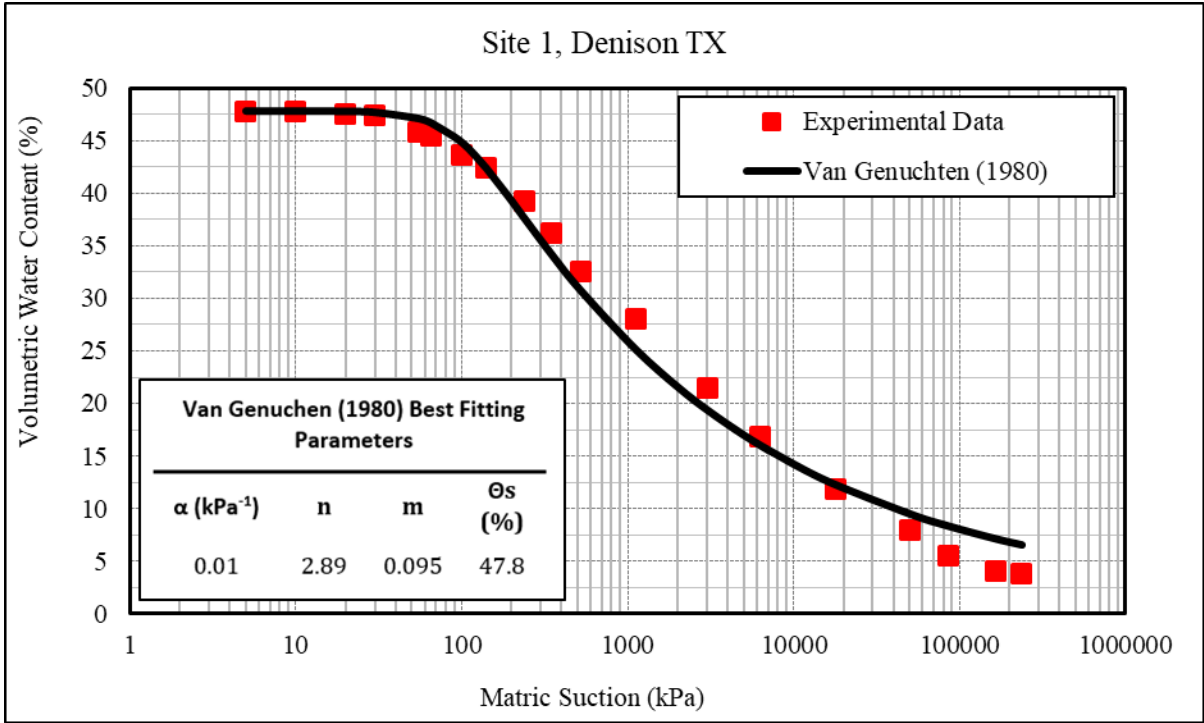


Figure 16. SWRC of Texas Site 1 soil using the Van Genuchten (8) model.

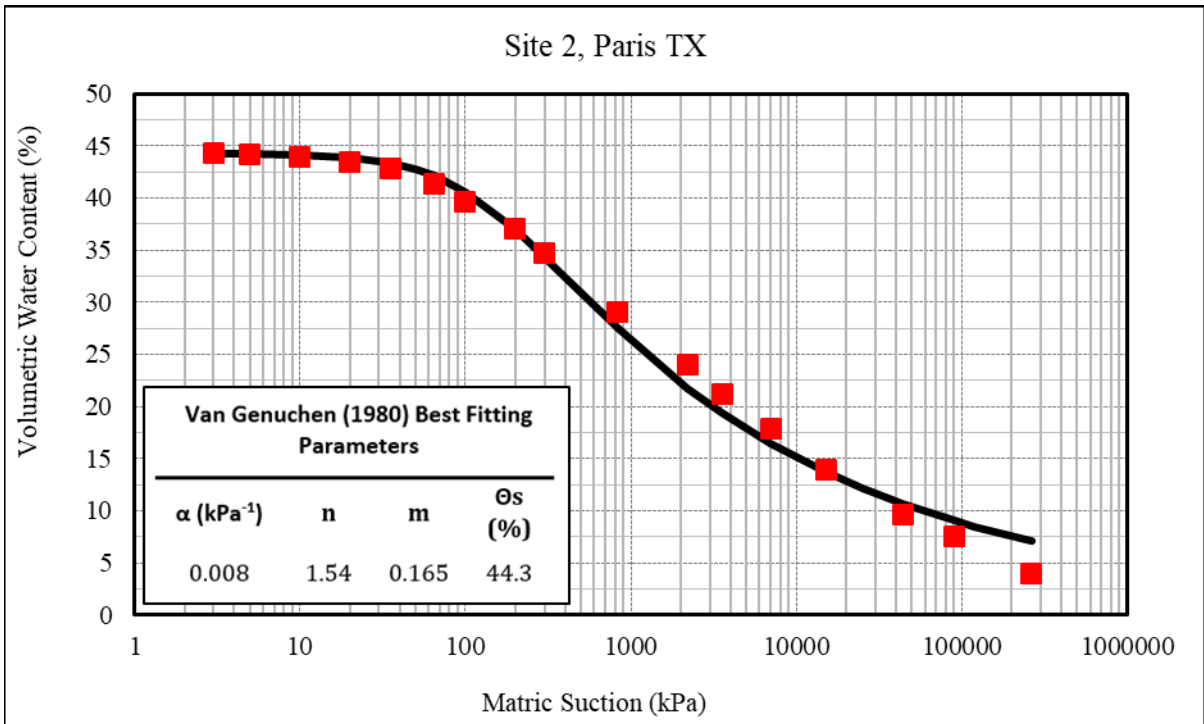


Figure 17. SWRC of Texas Site 2 soil using the Van Genuchten (8) model.

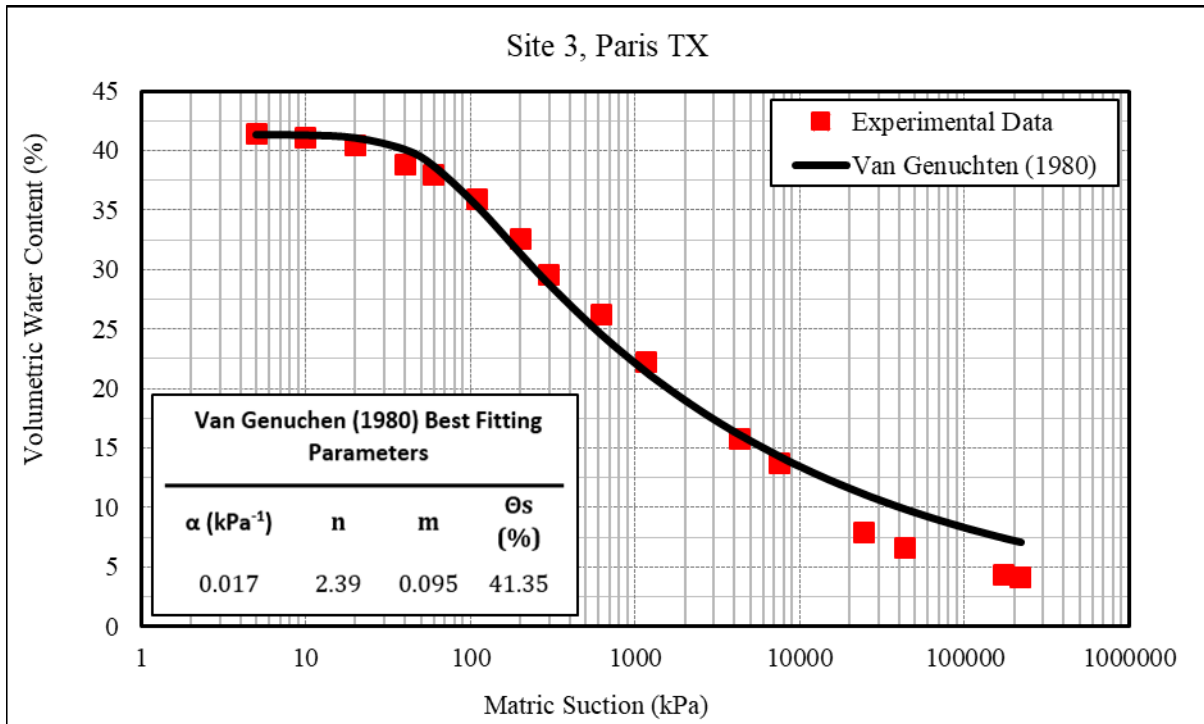


Figure 18. SWRC of Texas Site 3 soil using the Van Genuchten (8) model.

Texas Site 3 soil has a 41.35% maximum saturated volumetric water content and 4.3% residual volumetric water content. The air entry value of Site 3 is 40 kPa (5.80 psi). For Site 3, the best fitting parameters obtained from van Genuchten (8) model are $\alpha=0.017$ kPa⁻¹, $n=2.39$, $m=0.095$.

Louisiana Site 1 soil has a 42.22% maximum saturated volumetric water content and 6.4% residual volumetric water content. The air entry value of LA Site 1 soil is 38 kPa (5.51 psi). For Site 1, the best fitting parameters obtained from Van Genuchten (8) model are $\alpha=0.025$ kPa⁻¹, $n=1.7$, $m=0.116$.

Louisiana Site 2 soil has a 36.10% maximum saturated volumetric water content and 3.80% residual volumetric water content. The air entry value of LA Site 2 soil is 14 kPa (2.03 psi). For Site 2, the best fitting parameters obtained from Van Genuchten (8) model are $\alpha=0.053$ kPa⁻¹, $n=2.3$, $m=0.108$.

Louisiana Site 3 soil has a 47.16% maximum saturated volumetric water content and 7% residual volumetric water content. The air entry value of LA Site 3 soil is 65 kPa (9.43 psi). For Site 3, the best fitting parameters obtained from Van Genuchten (8) model are $\alpha=0.013$ kPa⁻¹, $n=2.87$, $m=0.094$.

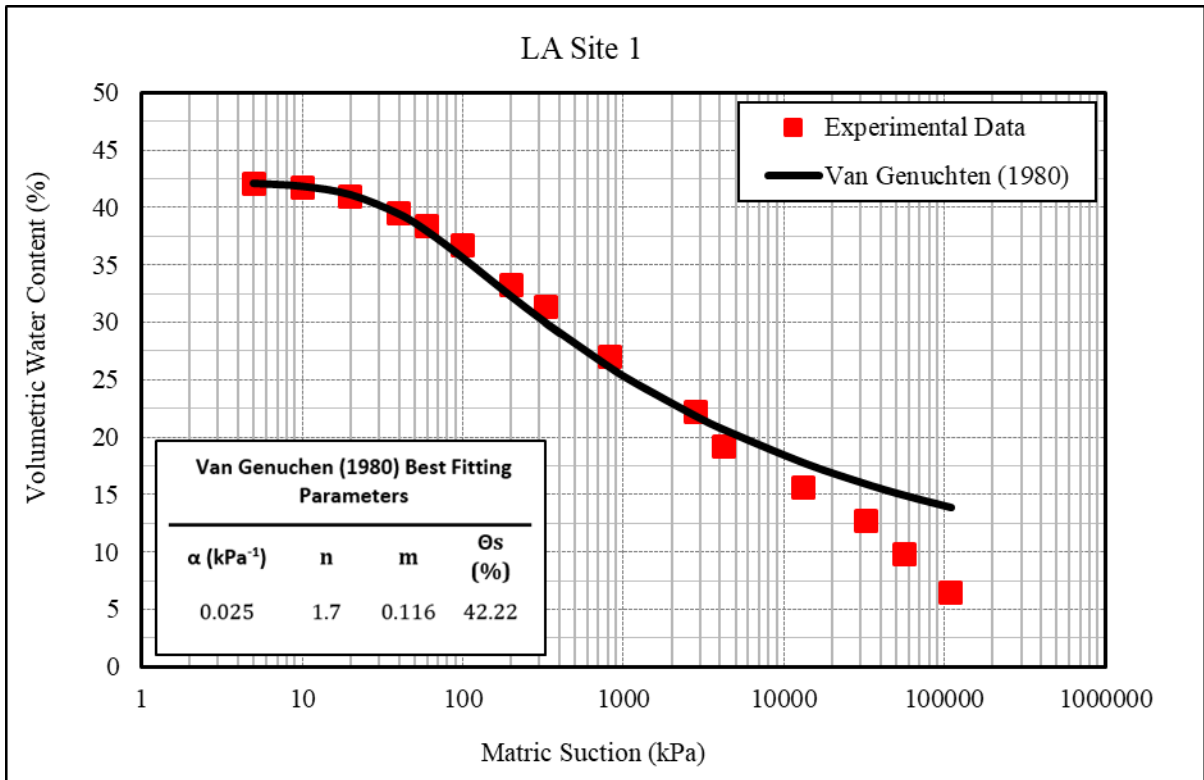


Figure 19. SWRC of Louisiana Site 1 soil using the Van Genuchten (8) model.

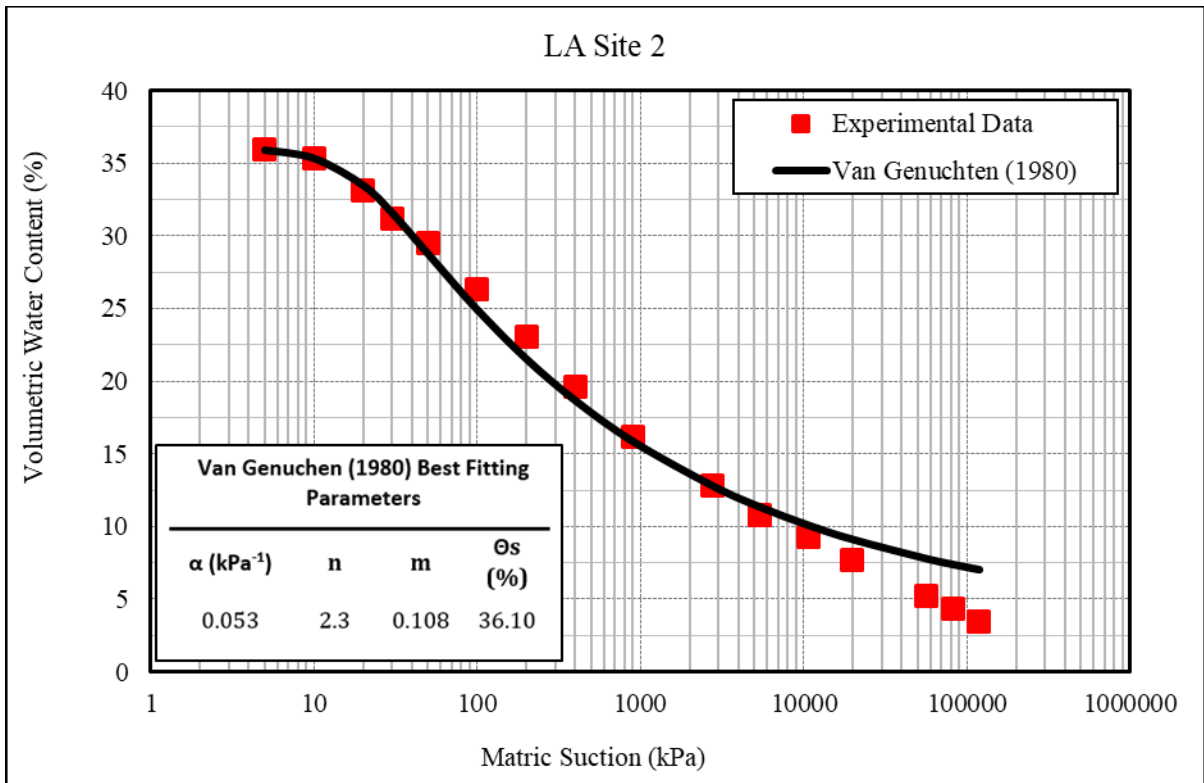


Figure 20. SWRC of Louisiana Site 2 soil using the Van Genuchten (8) model.

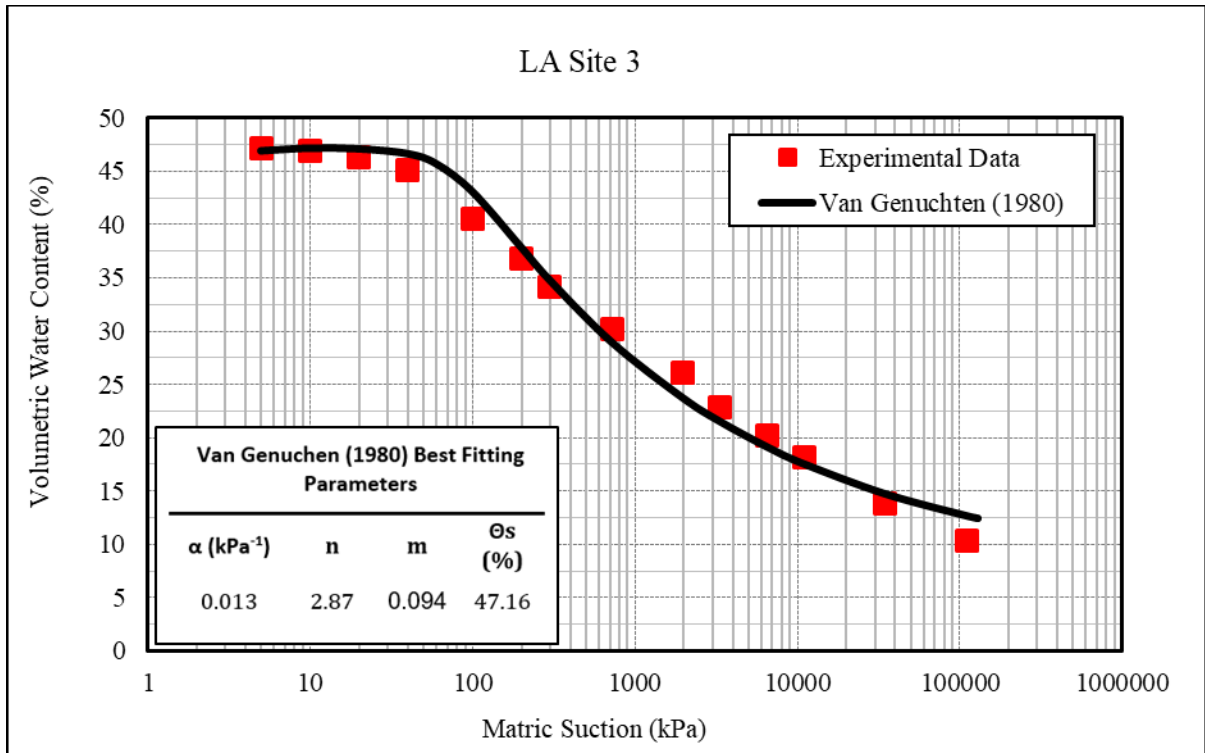


Figure 21. SWRC of Louisiana Site 3 soil using the Van Genuchten (8) model.

The obtained SWRC results from Tempe cell and WP4C apparatus indicate that tested soils have different saturated volumetric water content, drying path, air entry value, and residual volumetric water content. For Texas sites, Site 1 has the highest saturated volumetric water content of 47.8% while Site 2 and Site 3 has 44.3% and 41.35%, respectively. Moreover, Site 1 has high air entry value with 65 kPa. Similarly, Site 2 has 70 kPa air entry value. However, Site 3 has 40 kPa air entry value. For Louisiana sites, Site 3 has the highest saturated volumetric water content of 47.16% while Site 1 and Site 2 have 42.22% and 36.10%, respectively. Moreover, Site 3 has high air entry value with 70 kPa while Site 1 and Site 2 have 38 and 14 kPa air entry values, respectively. When the suction value is lower than the air entry value, it did not cause a change in water content whereas, with an increase in suction level the water content significantly drops to residual water content value. The high suction state represent the embankment soil conditions during summer season where the water content is low and the low suction levels represent the conditions after a rainfall event where the soil water content increases.

5.3. Fully Softened Strength and Correlations

Testing using the modified ring shear device is still ongoing due to initial delays in fabricating the bronze porous disks that are prescribed in the ASTM D6467-13, along with the long duration for testing one soil. For example, it can take 1-2 weeks to complete the fully softened tests at one site for the three normal effective stresses. Using the correlations developed by Stark and Eid (3) augmented by Stark et al. (10), Stark and Hussain (11), and Gamez and Stark (12), the fully softened shear stress envelopes for the three Texas sites are estimated in Figure 22 based on the CF and LL reported in Tables 2 and 3. Site 3 features the lowest clay fraction

and thus has a correspondingly higher fully softened shear stress envelope. Sites 2 and 3 feature similar clay fractions and liquid limits and hence have nearly identical FSS envelopes. Figure 23 provides the shear displacement curves, and Figure 24 shows the comparison of TX Site 1 to the Gamez and Stark (12) correlations, which consequently demonstrates the validity of the correlations to Texas soils.

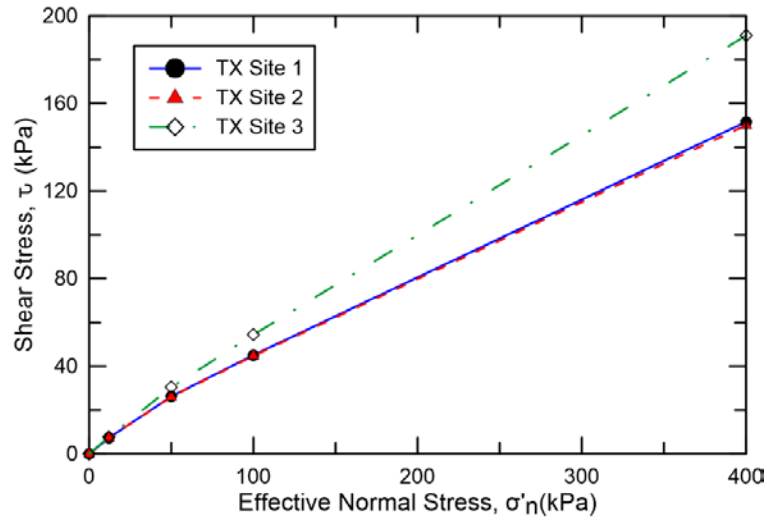


Figure 22. FSS correlation envelopes for Texas sites.

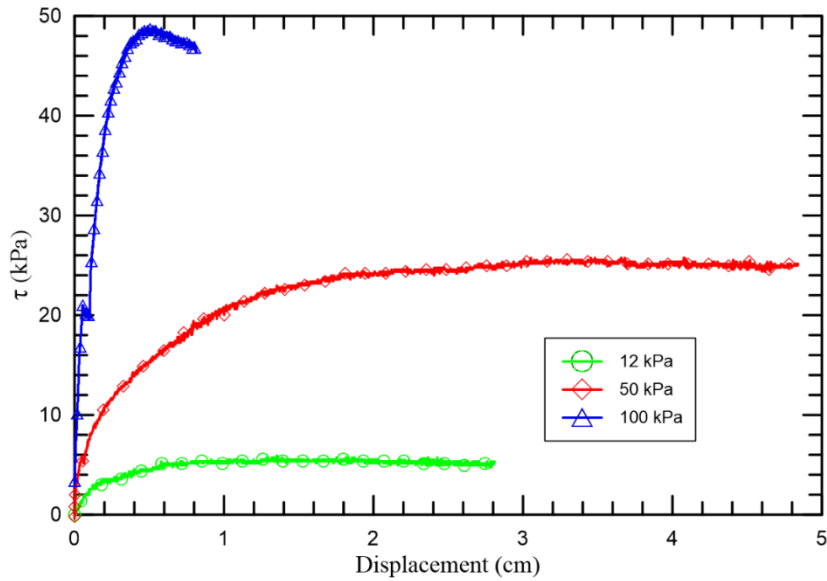


Figure 23. Ring shear test displacement and shear stress for Texas Site 1.

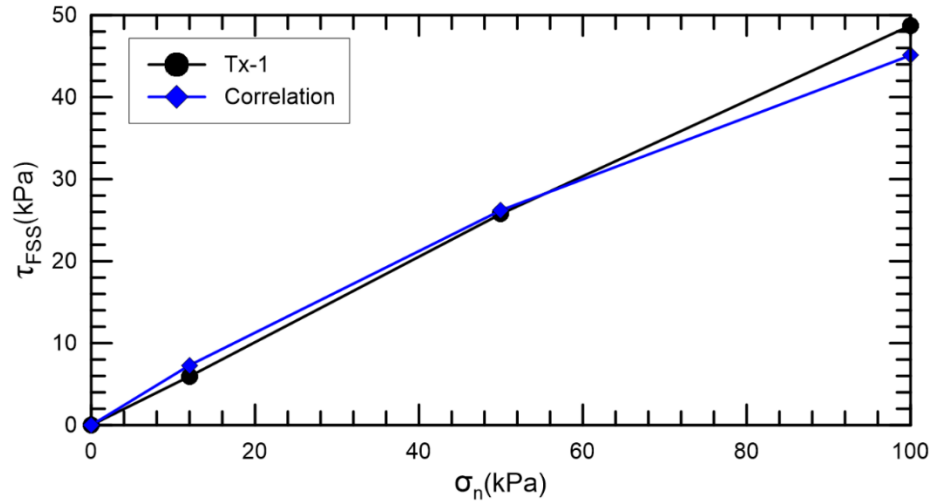


Figure 24. Fully softened shear strength envelope for Texas Site 1.

Results for the I-55 soils are presented in Figure 25(a), and results for the I-10 soils are displayed in Figure 25(b). During shearing, the test is left for 24 hours to ensure it reaches residual strengths. For Figure 25(a), the soils reach a peak shear stress or fully softened strength at less than 1 cm of displacement. With more displacement, the soil approaches a constant shear stress, which represents the residual strength. Similar behavior is observed for normal stresses of 12 kPa and 50 kPa in Figure 25(b). However, the peak strength is reached at 4 cm of displacement at a normal stress of 100 kPa.

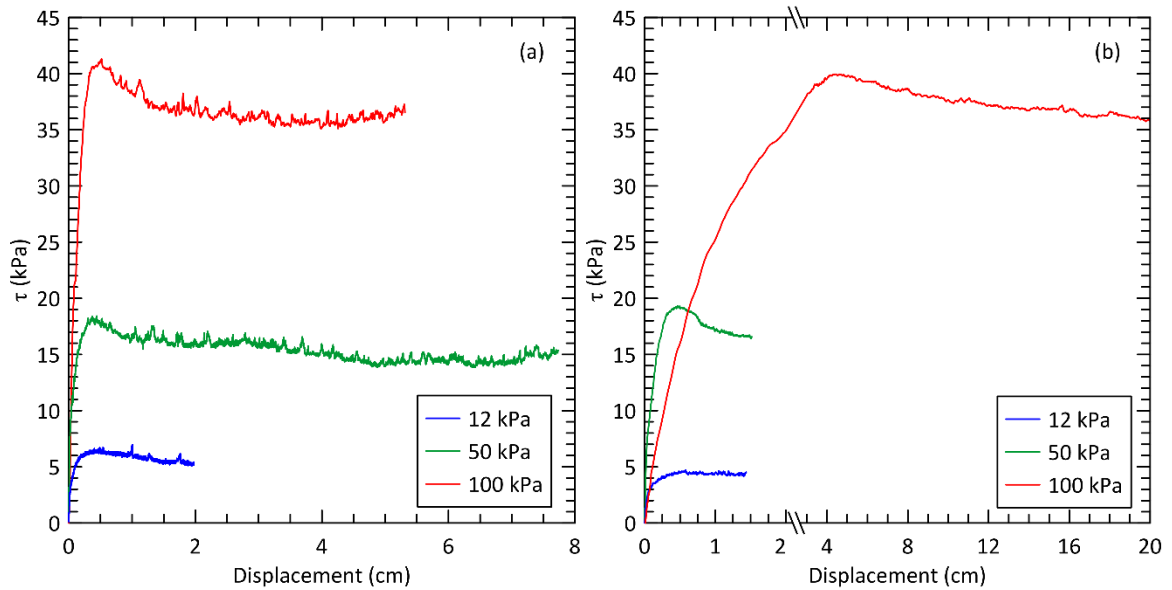


Figure 25. Ring shear test displacement and shear stress for Louisiana (a) I-10 and (b) I-55 sites.

The peak strength for each normal stress is used to develop the non-linear shear strength envelopes found in Figure 26. Both of the envelopes are plotted against the Gamez and Stark (7) correlation to compare the laboratory ring shear values. Gamez and Stark (7) provide the secant friction angles at 12 kPa, 50 kPa, and 100 kPa based on the soil clay size fraction and liquid limit. The CF and LL are 42% and 44% for I-55 sample and 55% and 48% for I-10

sample, respectively. This study and the correlation match for 12 kPa and 100 kPa but are slightly different for 50 kPa. The preliminary results demonstrate the efficacy of the Gamez and Stark (7) FSS correlations for Louisiana soils. The fully softened strength is currently not available for the Lake Nantachie site because of the limited amount of soil.

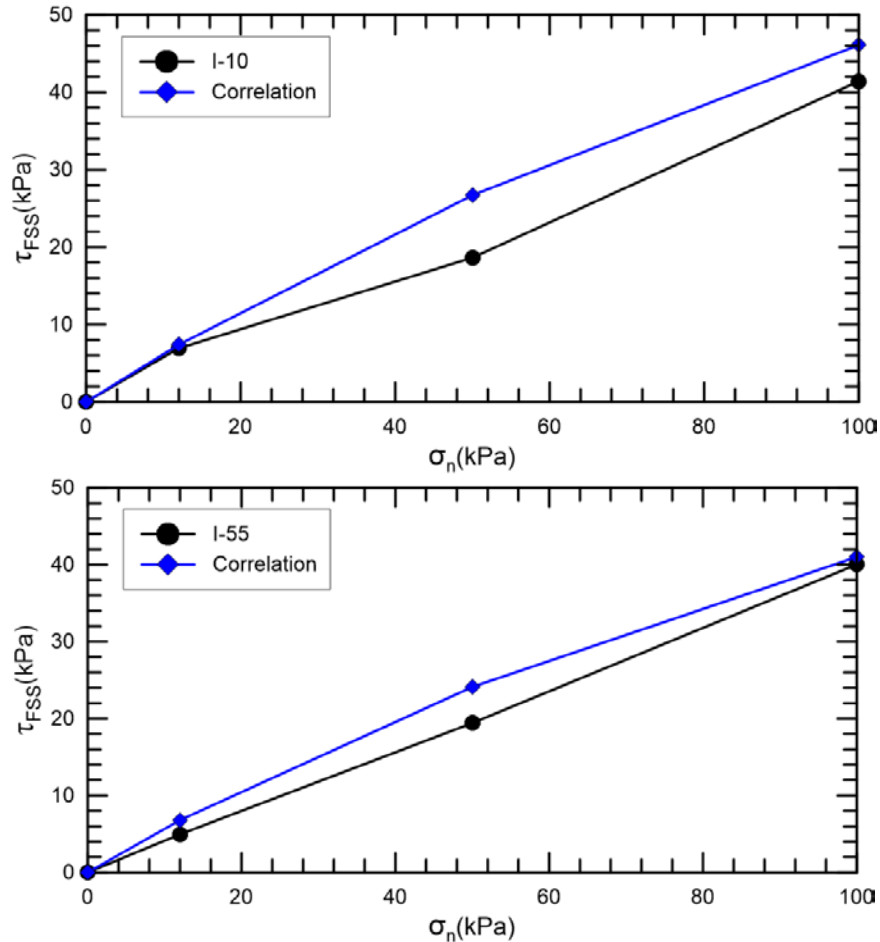


Figure 26. Fully softened shear strength envelope for Louisiana (top) I-10 and (bottom) I-55 sites.

5.4. Climate Coupled Modeling of Highway Embankments

To evaluate the effects of climate on high plasticity embankments, a climate-coupled model was designed. Using an embankment in Baton Rouge, LA as a case study, the effects of climate coupling on compacted clay embankments was investigated using the finite element packages in GeoStudio 2018. The site in Baton Rouge is not one of the three aforementioned locations and was selected because of high quality weather station data was available less than 2 miles, which was not the case for sites in Texas. The embankment is about 8 m in height with slopes of 3H:1V. The embankment consists of silty clay to high plasticity clay, similar to the other embankments tested in this project. Climatic data was obtained from the Louisiana State University Agrilclimatic Center (Figure 27), which has a network of weather stations across the state. The model was run for approximately two years, with the first year used as spin-up time into realistic physical conditions.

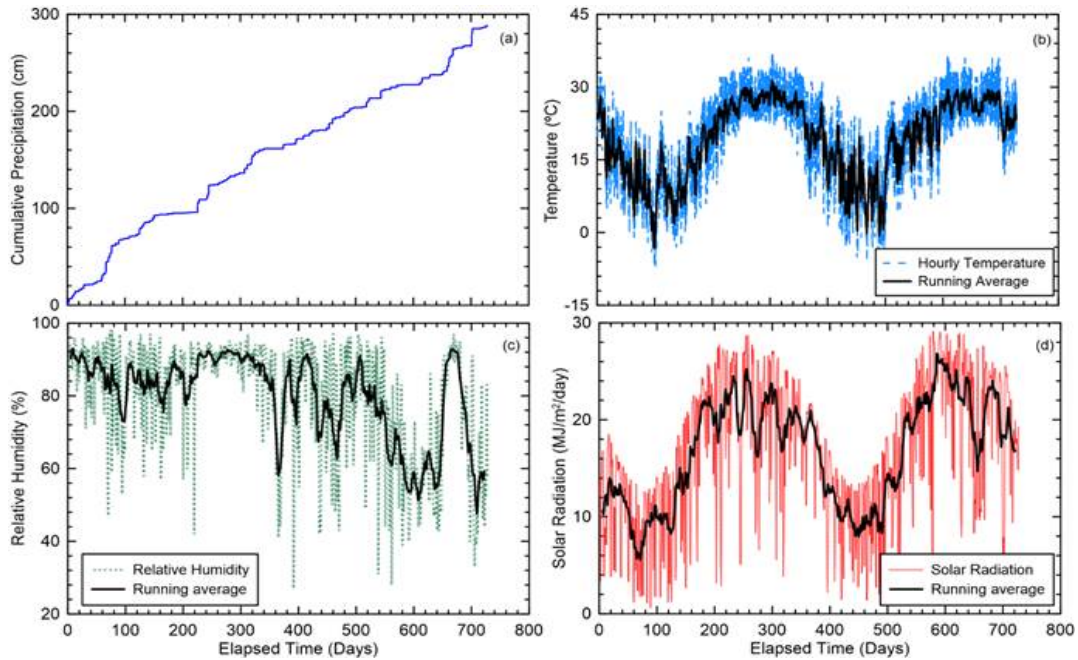


Figure 27. Climatic data obtained from the Louisiana State University Agrilimatic Data System.

Coupling the climatic data to the embankment illustrates the elevated pore water pressures developed during rain events. As seen in Figure 28, the phreatic surface in the high plasticity embankment progresses through the core of the high plasticity embankment and correspondingly raises pore water pressures on the slope faces. Through the model run, a variety of conditions were present, including drought and heavy precipitation. Following heavy precipitation events, the high plasticity embankments seem to stay saturated longer than initially expected.

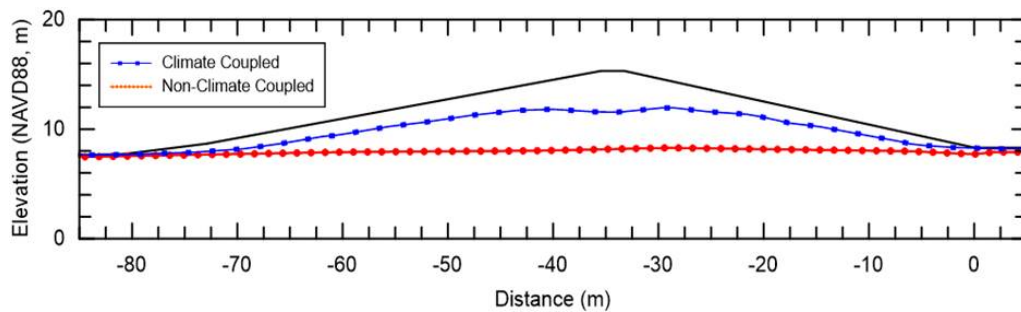


Figure 28. Elevated phreatic surface location in climate coupled model.

5.5. Framework for Evaluating Stability of Highway Embankment Slopes

Table 6 shows again the risk classification from Burns et al. (2). This framework defines the probability of slope instability based on index properties of the soil, i.e. higher plasticity index and clay content results in lower shear strengths and hence high failure probabilities. The research results from ring shear testing substantiate that higher PI and CF soils are less stable because of lower FSS envelopes. To further expand on Burns et al. (2) system, the framework proposed herein is the first step in creating a heat map of the stability of highway embankments

that integrates shear strength, embankment geometry, and water infiltration. Hundreds of miles of highway embankments exist in Texas and Louisiana. A framework that can accurately predict when and where a failure is currently elusive because of the variability in soil properties, e.g., unsaturated properties, peak or fully softened strength, and presence of tension cracks. However, a classification system that is site specific to a DOT district or region can be developed based on the proposed framework. The outcome is to take representative slopes with engineering properties and provide likelihood failure with rainfall totals.

Table 6. Embankment failure risk classification system (2).

Risk Level	Clay Content (%)	Plasticity Index	Liquid Limit	Net Smectite	Chance Of Failure
High	>47	>29	>54	>33	85-90
Intermediate	32-47	16-29	36-54	18-33	55-60
Low	<32	<16	<36	<18	<5

The framework starts with estimating the fully softened shear strength based on the Stark et al. (13) correlation. It is assumed the soil reaches a fully softened strength in order for the embankment to fail. This does not account for the time to reach fully softened strength, which means “younger” embankments are less likely to fail than embankments that were built over 20 years ago. The unsaturated and saturated hydraulic properties from both Louisiana and Texas sites will be leveraged to predict the pore-water pressure response due to precipitation events. With the advent of high-quality meteorological data, coupled SEEP/W and SLOPE/W models can be used to determine the conditions at which the factor of safety approaches unity (1.0). The I-55 Hammond site is used as an example of the workflow. The geometry, shear strength, and hydraulic properties are input into the GeoStudio suite of SLOPE/W and SEEP/W. Hindcast simulations of meteorological data is used to constrain the rainfall duration and intensity that causes the factor of safety to approach unity. In particular, rainfall infiltration will convert the unsaturated soil to saturated conditions and ultimately raise the pore-water pressures such that a shallow failure is imminent. The rainfall characteristics that lead to failure will be converted into a range of precipitation, which will be compared to weather forecasts. As a result, when weather forecasts and measured rainfall amounts approach values predicted in the predictive framework, it is likely that a shallow slide occurred. In this framework, the initial matric suction profile of the embankment is accounted for in the SEEP/W model, i.e., a period of limited rainfall will result in higher matric suction profiles and hence lower pore-water pressures. The time for the soils to reach a fully softened is not currently incorporated in this framework and thus is an area of future research. The predictive framework will also need case studies to validate the hypothesis that the weather forecasts can be used as a first order attempt to anticipate slope failures using site specific fully softened correlations and hydraulic properties.

Rehabilitation techniques were obtained from discussions with LADOTD engineers. In particular, Zhang et al. (13) recommendations are the current standard to repair highway embankment slopes. While LADOTD has this standard repair, it is recommended to re-evaluate the use of new technologies, such as the Tencate H2Ri geotextile, Hayward Baker ground improvement techniques, and UTA team recommendations for lime stabilized soils.

6. CONCLUSIONS

The current study found that literature and experiments on Louisiana highway embankment failures was lacking. Failures predominantly occurred in recent river alluvium and in Pleistocene Prairie clays (2). Failures in Louisiana which have occurred post-publication of the 1990 embankment report are numerous and poorly documented. Through collaboration with LADOTD, the current project has produced a failure database which can be used to further document and study embankment failures in Louisiana and to help predict where they are most likely to occur. Rehabilitation techniques were obtained from discussions with LADOTD engineers. In particular, Zhang et al. (13) recommendations are the current standard to repair highway embankment slopes. The efficacy and cost-effectiveness of this method has not been investigated with over the course of the embankment service life. While LADOTD has this standard repair, it is recommended to re-evaluate the use of new technologies, such as the Tencate H2Ri geotextile, Hayward Baker ground improvement techniques, and UTA team recommendations for lime stabilized soils. The ring shear tests are demonstrating that the Gamez and Stark (12) correlations are applicable to Texas and Louisiana soils. The unsaturated hydraulic properties of Texas and Louisiana soils were evaluated. The air entry values vary from 0.013 to 0.053 kPa⁻¹ in Louisiana and from 0.008 to 0.01 kPa⁻¹. The implications of this wide range are that the matric suction pressure required to saturate and desaturate the soil controls also the pore-water pressure build-up during a rainfall event. Climate coupled modeling provides the ability to visualize transient pore-water pressure development in response to climatic conditions and should be utilized in the design process and back analysis of embankment failures of high plasticity clays. During the design process, the effect of desiccation crack development and subsequent hydraulic conductivity increase should be considered under various climatic scenarios. A first order predictive framework is proposed on the lessons learned, but case studies are need to verify and further expand into a heat map.

7. RECOMMENDATIONS

The recommendations for future work based on the findings and lessons learned in this study are the following:

1. Develop a central online form for headquarters and local districts to document highway embankment failures, repairs, and new construction. This will assist in asset management, which is a key focus of the Federal Highway Administration.
2. Employ street viewer equipment to rapidly assess the condition of highway embankments. For example, the Google street viewer can take panoramic images at high speeds. This allows the LADOTD to perform assessments of highway infrastructure and subsequently develop algorithms to identify failures.
3. Further extend the fully softened shear strength and unsaturated hydraulic testing of Texas and Louisiana soils.
4. Instrument field sites across Texas and Louisiana to understand the pore-water pressure regime based on seasonal climate variations and short-term meteorological events. This information will help guide the next-generation of the predictive model.
5. Construct a full-scale highway embankment and monitor the shear strength with time to understand how fast the values decrease with the number of wetting-drying cycles.
6. Implement field test sites of the Tencate Mirafi H2Ri as a means for repairing failed slopes. It is postulated that the active drainage in these geotextiles will enhance the service life of the highway embankment.

REFERENCES

1. Matson, G.C. (1917). Louisiana Clays. Contributions to Economic Geology. Washington, D.C., United States Geological Survey.
2. Burns, S. F., Hadley, W. O., Mutchler, J. W., Smith, S. M., Siddiqui, A., and M. Hernandez (1990). "Development of Design Criteria for the Prevention of Slope Failures." Louisiana Transportation Research Center.
3. Stark, T. D. and H.T. Eid (1993). "Modified Bromhead ring shear apparatus." *Geotech. Test. J.*, 16(1), 100–107.
4. Fredlund, D. G. and H. Rahardjo (1993). "Soil Mechanics for Unsaturated Soils." Wiley, New York.
5. Fredlund, D.G. (2006). "The Terzaghi Lecture: Unsaturated soil mechanics in engineering practice." *Journal of Geotechnical and Geoenvironmental Engineering*, vol. 132(3), pp. 286–321.
6. Hilf, J.W. (1956). "An Investigation of Pore-Water Pressure in Compacted Cohesive Soils." Tech. Memo. 654, U.S. Department of the Interior, Bureau of Reclamation Design and construction Div, Denver, Colorado.
7. Brooks, R.H., and A.T. Corey (1964). "Hydraulic properties of porous media." *Hydrology Papers Colorado State University*, Fort Collins.
8. Van Genuchten, M.T. (1980). "A closed-form equation for predicting the hydraulic conductivity of unsaturated soils." *Soil Science Society American Journal*, vol. 44, pp.892–898.
9. Fredlund, D.G and A. Xing (1994). "Equations for the soil water characteristic curve." *Canadian Geotechnical Journal*, vol. 31, pp. 521-532.
10. Stark, T.D., Hangseok C., and S. McCone (2005). "Drained Shear Strength Parameters for Analysis of Landslides." *Journal of Geotechnical and Geoenvironmental Engineering*, 131(5), 575-588.
11. Stark, T.D. and M. Hussain (2013). "Empirical correlations: Drained shear strength for slope stability analyses." *ASCE Journal of Geotechnical and Geoenvironmental Engineering*, June 2013, vol. 139(6), pp. 853–862.
12. Gamez, J. and T.D. Stark (2014). "Fully Softened Shear Strength at Low Stresses for Levee and Embankment Design." *ASCE Journal of Geotechnical and Geoenvironmental Engineering*, June. 2014, pp. 06014010-1-06014010-6.
13. Zhang, Z., Farrag, K., and M. Morvant. (2003). "Evaluation of the Effect of Synthetic Fibers and Nonwoven Geotextile Reinforcement on the Stability of Heavy Clay Embankments". Report No. 373, Louisiana Transportation Research Center.